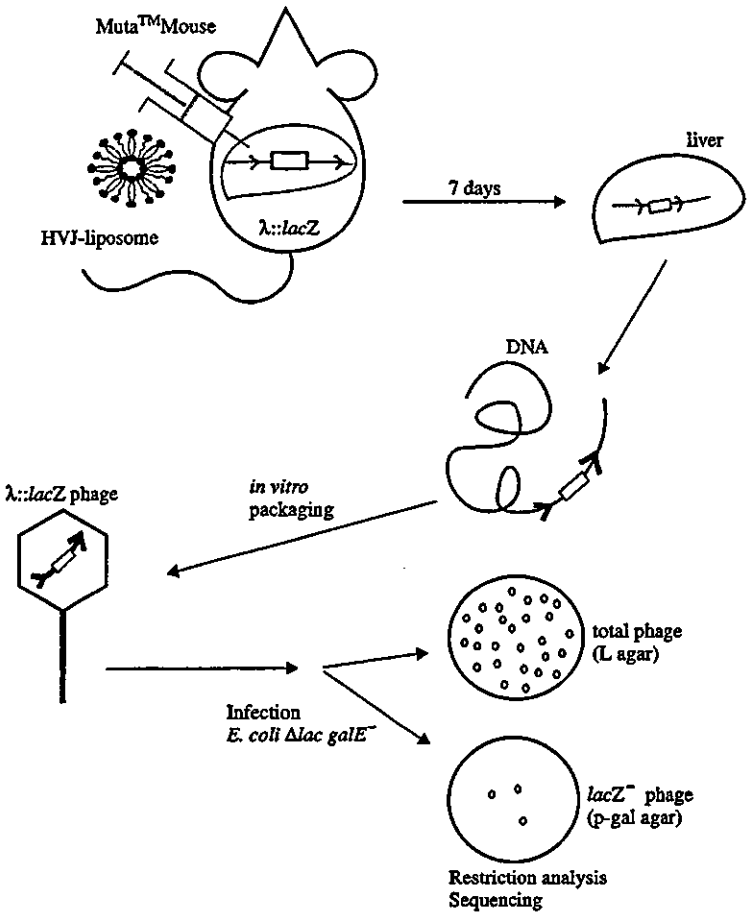

Figure 1. Experimental steps. Steps for gene targeting with RNA/DNA oligonucleotide chimera *in vivo* and detection of sequence changes with mutation reporter mice

In contrast, it is much less efficient and imprecise in mammalian cells [2], although it is now widely used to modify mouse genomes at the germ-line level with embryonic stem (ES) cells. In order to employ this method for targeted mutation correction in somatic cells, a high frequency and a high precision are required.

A special form of oligonucleotides was reported to be able to correct a point mutation with a high efficiency in cultured rodent cells, in the body of mice and rats, and in plants [3–6]. The efficiency of correction in the liver of rats following their tail-vein injection together with polyethylenimine was reported to be higher than 10% [3]. These oligonucleotides have a short double-stranded structure with 20–30 bp homology with the target and are characterized by the presence, in one strand of the homologous region, of 2′-*O*-methyl RNA, which is believed to be important in initiating homologous pairing and stabilizing the structure [7,8]. However, molecular mechanisms underlying this technique are not yet fully understood. Some laboratories have reported failure to reproduce the high efficiency [9–12].

We wished to sensitively detect gene correction, if any, with these oligonucleotides *in vivo*. In order to avoid the potential drawbacks of the polymerase chain reaction (PCR)-based assays, we employed a mutation reporter system with transgenic mice, which has been used for sensitive and quantitative measurement of mutation frequency *in vivo* [13]. This system has been used successfully to detect mutation induction by various agents interacting with DNA, which include *N*-methyl-*N*-nitrosourea in various organs [14], which included the liver [15]. For gene delivery, we carried out direct injection into the liver lobe with HVJ-AVE liposome, which has proved to be a reliable procedure for gene delivery and expression in liver: the transgene was expressed in 30% of the treated cells [16]. We found that the gene correction efficiency with the RNA/DNA oligonucleotides was less than 1/20 000 in this system. This is the first report of a failure *in vivo* using a sensitive reporter system.

Materials and methods

Bacteria, bacteriophages and plasmids

The strains of bacteria *Escherichia coli*, the strains of bacteriophage lambda, and the plasmids used are listed in Table 1. BIK12001 was used for titration of lambda

phage and for measurement of lacZ-negative lambda by phenyl-beta-D-galactoside (p-gal) selection. BIK2206 was used for confirmation, with 5-bromo-4-chloro-3-indolyl-beta-D-galactose (X-gal), of the LacZ-negative phenotype of the phage selected with p-gal.

LIA25 and LIA26 were derived from lambda gt10*lacZ* by introducing a G to C change at position 2210 and A to C change at position 2211 of *lacZ*, respectively. We first cloned its lacZ gene and the flanking region into a plasmid in two steps (Table 1; pNY17 and pNY19). We introduced the mutations by site-directed mutagenesis (pIA1 and pIA2) and transferred the mutations back to lambda by homologous recombination *in vivo* as follows. The site-directed mutagenesis was carried out with pNY19 using the QuickChange XL site-directed mutagenesis kit (Stratagene, CA, USA). To construct pIA1, primers ML2-3 (ctggtcgctggggaatcaatcaggccacggcgc) and ML2-4 (gcgccgtggcctgattgattccccagcgaccag) were used; to construct pIA2, ML3-3 (catctggtcgctggggaatgcatcaggccacggcgctaatc) and ML3-4 (gattagcgccgtggcctgatgcattccccagcgaccagatg) were used. The *lacZ* region (1st to 3127th bp) was sequenced to verify the presence of the designed mutation and the absence of any other sequence change. Sequencing was performed with the ABI PRISM BigDye Terminator v3.0 ready reaction cycle sequencing kit (Applied Biosystems, CA, USA) on a GeneAmp PCR system 9600 (PE) (Applied Biosystems) with the sequencing primer. The recombinational transfer of the mutation between lambda and plasmids was carried out as follows. Cells of BIK12033 or BIK12034 were grown to about $3-5 \times 10^8$ cells/ml ($OD_{600} = 0.3$) in LB (10 g bactotrypton, 5 g yeast extract, 10 g of NaCl per liter) containing chloramphenicol (20 μg/ml), 0.2% maltose and 10 mM $MgSO_4$. The bacteriophage LIA22 was adsorbed to the cells at a multiplicity of 1.0 at 37 °C for 15 min. The mixture was shaken at 37 °C until the OD_{600} dropped below 0.3. $CHCl_3$ was added to the mixture, which was shaken for 30 s. The mixture was centrifuged, and the supernatant was recovered. The supernatant were assayed on agar plates containing p-gal, as detailed below. The plaques on the p-gal plates were isolated and analyzed for the designed sequence change.

P-gal selection

The *lacZ*-negative phage particles were detected by positive selection [17,18]. Cells of BIK12001 were grown to $OD_{600} = 1.0$ in LB containing ampicillin (50 μg/ml), kanamycin (20 μg/ml) and 0.2% maltose at 37 °C. The culture was centrifuged at 3500 rpm for 15 min at 4 °C. The pellets were dissolved into half a volume of LB containing 10 mM $MgSO_4$. The phage sample was adsorbed to BIK12001 cells at room temperature for 20 min. For estimation of total number of phage, 2.5 ml of molten 1/4LB top agar (5 g of LB broth base (Gibco BRL, Rockville, MD, USA), 6.4 g of NaCl, 7.5 g of bactoagar, per liter) were added to 0.25 ml of the mixture of BIK12001 cells and phage and the mixture was poured onto a 1/4 LB plate (5 g LB broth base (Gibco BRL), 6.4 g NaCl, 15 g bactoagar, per liter). For estimation of the number of *lacZ*-negative phages, 2 ml of the mixture of BIK12001 cells and phage and 22 ml of molten 1/4LB top agar containing 0.3% p-gal (Sigma Chemical Co., MO, USA) were mixed and poured onto four 1/4 LB plates. The plates were incubated at 37 °C for 12 h.

Transfer of RNA/DNA oligonucleotides to mouse liver

All the animal experimental protocols were approved and carried out in accordance with the guidelines of the

Table 1. Bacterial strains, plasmids, and bacteriophage strains

Strain	Genotype	Source/reference
Bacteria (*Escherichia coli*)		
BIK12001	Strain C, deletion *lacgalE*$^-$	T. Suzuki/Manufacturer's manual
BIK2206	Strain C, deletion *lac*	Manufacturer's manual
BIK806	A *recD::Tn*10 derivative of AB1157 of K-12	[14]
BIK12033	BIK806 [pIA1]	This work
BIK12034	BIK806 [pIA2]	This work
Bacteriophage lambda		
LIA22	λgt10 *imm434::lacZ*	Recovered from MutaMouse/ [12]
LIA25	λgt10 *imm434::lacZ*$^-$, Glu461Gln (GAA to CAA)	This work
LIA26	λgt10 *imm434::lacZ*$^-$, Glu461Ala (GAA to GCA)	This work
Plasmids		
pIK153	p15A origin, *cml* and a multiple cloning site from pUC119	[15]
pNY17	*cml lacZ*$^+$	BglII-BamHI fragment of λgt10 *lacZ* (carrying lacZ gene) was inserted into BamHI site of pIK153.
pNY19	*cml lacZ*$^+$	SacI-SmaI fragment of pNY17 (carrying origin, Cm^r and *lacZ*) gene and SmaI fragment of λgt10 *acZ* (carrying part of *imm434*) were ligated.
pIA1	*cml lacZ*$^-$, Glu461Gln (GAA to CAA)	Point mutation that LZ-2 is expected to induce was introduced to pNY19 by site-directed mutagenesis.
pIA2	*cml lacZ*$^-$, Glu461 Ala (GAA to GCA)	Point mutation that LZ-3 is expected to induce was introduced into pNY19 by site-directed mutagenesis.

Animal Committee of Osaka University. Male MutaMice, 8 weeks of age, were obtained from Covance Research Products Inc. (Denver, PA, USA). The mice were housed five per cage and allowed access to food and water *ad libitum*. RNA/DNA chimera oligonucleotides were synthesized by Applied Biosystems, Inc. (ABI, Foster City, CA, USA) and purified by high-performance liquid chromatography (HPLC). This purification was done by ABI also. The purity of full-length LZ-2 and LZ-3 was 80% and 70%, respectively, according to the manufacturer. The oligonucleotide was incorporated into liposomes as detailed previously [16]. In brief, the oligonucleotide (300 μg) was incorporated into liposomes prepared from 10 mg of lipids (artificial viral envelope, AVE), and the resulting liposomes were fused with inactivated hemagglutinating virus of Japan (HVJ). These HVJ-AVE liposome complexes were then separated from free HVJ by sucrose density gradient centrifugation. The final HVJ-AVE liposome volume was approximately 500 μl, and its total volume was adjusted to 900 μl with saline. The mice were anesthetized and underwent midline incision. A large lobe of the liver was exposed, and 300 μl of HVJ-AVE liposomes containing 20 μg of the oligonucleotide were injected directly into the lobe with a 1-ml syringe with a 30-gauge needle, and the incision was sutured.

Transfer of fluorescence-labeled oligodeoxynucleotides

Fluorescence isothiocyanate-labeled oligodeoxynucleotides (FITC-labeled oligonucleotides) (5′-FITC-TCCATGACGTTCCTGATGCT-3′) were synthesized by Hokkaido System Science Co., Ltd. (Sapporo, Japan). The FITC-oligonucleotides (31 μg, 4.6 nmol, which is the same mole quantity as the RNA/DNA chimeric oligonucleotides) in 200 μl balanced salt solution (137 mM NaCl, 10 mM KCl, 10 mM Tris-HCl, pH 7.6) were mixed with 10 mg of dried lipids to prepare HVJ anionic liposomes as described above. Then, 200 μl of the HVJ-AVE liposome containing the FITC-oligonucleotides were injected directly into a liver lobe of a mouse as described above. As a negative control, HVJ-AVE liposomes containing an unlabeled form of the oligonucleotides were prepared and introduced similarly. Twenty-four hours after introduction, the livers were removed and fixed with 4% paraformaldehyde. Frozen sections (5 μm thick) were observed under a fluorescence microscope.

Isolation of DNA, recovery of lambda phage, and measurement of mutant frequency

Seven days after injection, the mice were sacrificed, and the lobe of the liver was excised and stored frozen at −80 °C. DNA was isolated from the liver tissue with a RecoverEase™ DNA isolation kit (Stratagene) following the manual. The starting amount of the liver was about 30 mg. Lambda gt10*lacZ* particles were recovered from the isolated genomic DNA with packaging extracts (Transpack packaging extract; Stratagene). The *lacZ*-negative mutants were detected by p-gal selection as described above. Every plaque on the selective agar was recovered in 100 μl of SM buffer (50 mM Tris-HCl, pH 7.5, 10 mM $MgSO_4$, 100 mM NaCl, 0.01% gelatin). To verify their *lacZ*-negative phenotype, these phage isolates were assayed on agar with X-gal by a spot assay as follows. BIK2206 was grown in LB containing ampicillin (50 μg/ml) and tetracycline (10 μg/ml) to $OD_{600} = 1.0$. The culture was centrifuged at 3500 rpm for 15 min. The pellets were dissolved in half the initial volume of LB containing 10 mM $MgSO_4$. Then, 1.25 ml of the culture were mixed with 6 ml of molten LB/MM agar (100 ml LB medium, 0.75 g bactoagar, 10 mM $MgSO_4$, 0.2% maltose, 0.35 mg/ml X-gal) and spread on agar. A 10-μl aliquot of each phage sample was spotted. The plates were incubated overnight at 37 °C. The mutant frequency was estimated by dividing the number of plaque-forming units (pfu) on the selective plate (as verified with X-gal) by the number of total pfu on 1/4 LB agar. The fraction of false positive clones was less than 1/4.

Analysis of mutant DNA

The *lacZ*-negative lambda DNA from the mice that had been treated with LZ-3 was analyzed with restriction enzyme after PCR. The primers LG-1 (5′ TACCGGCGATGAGCGAAC 3′) and LG-2 (5′ CTCCAGGTAGCGAAAGCC 3′) were used to amplify the target region of the lambda phage in a thermal cycler (Robocycler; Stratagene) with DNA polymerase Ex. Taq (TAKARA BIO Inc. Shiga, Japan) as follows: 94 °C, 2′; 94 °C, 30″; 56 °C, 30″; 72 °C, 30″, 30 cycles; 72 °C, 2′. The PCR product of 288 bp was purified by ethanol/sodium precipitation. The fragment was digested with TfiI (New England Biolabs, Beverly, MA, USA) at 65 °C and analyzed by agarose electrophoresis. The mutant sequence is resistant to TfiI, while the wild-type sequence is sensitive, yielding 204 and 84 bp fragments. DNA from the mice that had received LZ-2 was analyzed by sequencing. The PCR was carried out to amplify the target region with primers AdG-3 (5′ CTCTATCGTGCGGTGGTTG 3′) and AdG-4 (5′ CGGGGATACTGACGAAACG 3′). The amplification was checked by electrophoresis of 5 μl of the products. The PCR products were purified with the QIAquick PCR purification kit (Qiagen, Valencia, CA, USA). Cycle sequencing was performed with the ABI PRISM BigDye Terminator v3.0 ready reaction cycle sequencing Kit (Applied Biosystems) on a GeneAmp PCR system 9600 (PE) (Applied Biosystems) with the same primers.

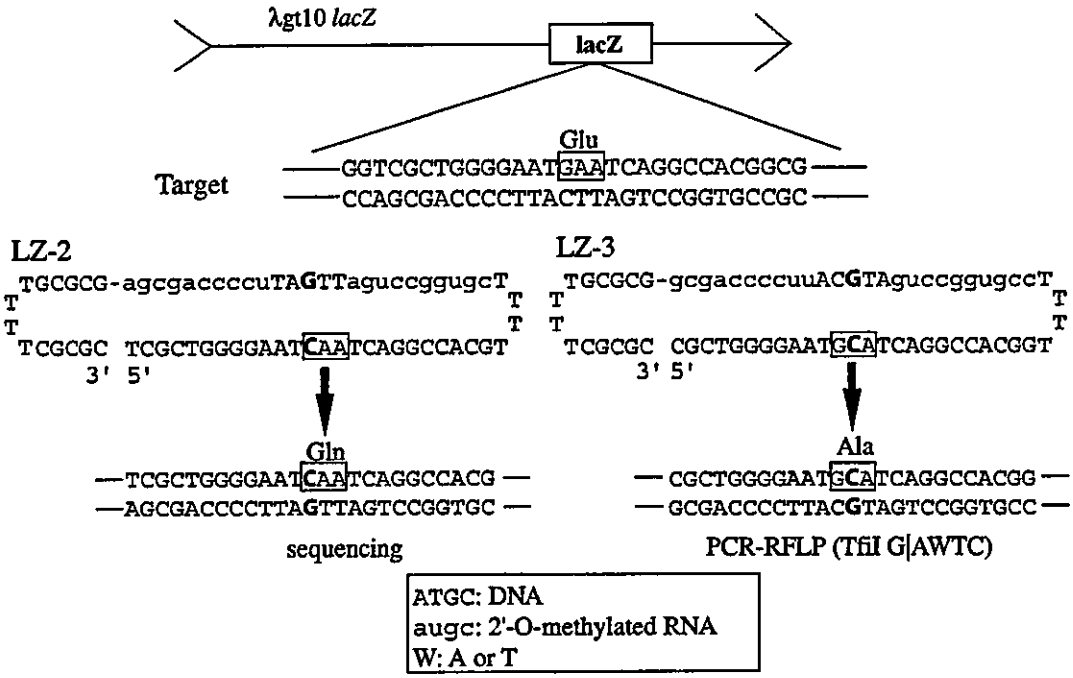

Figure 2. Design of gene targeting with RNA/DNA oligonucleotides. The Glu[460] codon of the *lacZ* gene for the active site of beta-galactosidase is *boxed* in *gray*. LZ-2 and LZ-3 RNA/DNA oligonucleotide chimera sequences were designed to induce a G/C to C/G and a A/T to C/G mutation, respectively. The mutant sequence is indicated in *bold*. *Capital letters* indicate DNA residues, while *lower-case letters* indicate 2'-*O*-methylated RNA residues

Results

A system for detection of gene correction *in vivo*

Figure 1 illustrates our experimental design to sensitively detect gene correction (targeted mutagenesis) *in vivo* without depending on PCR. Muta™Mouse, a transgenic mouse developed as a mutation reporter [13], carries approximately 40 copies of λgt10*lacZ* on a chromosome [19]. The target of gene correction with the RNA/DNA oligonucleotides is the region of its wild-type *lacZ* gene coding the active site of beta-galactosidase. After the induction of chimeric oligonucleotides, the DNA is isolated and, after *in vitro* packaging, recovered in a bacteriophage particle. The *lacZ*-negative mutant phage is selected on *Escherichia coli* mutants defective in the *galE* gene on a special agar plate containing p-gal. This chemical is converted by beta-galactosidase into a toxic intermediate, which accumulates in the absence of GalE protein to kill the cell. The ratio of the mutant plaque formers to the total plaque formers is taken as the fraction of the mutated gene. The mutant gene is further analyzed by restriction and sequencing.

For gene delivery *in vivo*, we used a liposome composed of HVJ (hemagglutinating virus of Japan, also called Sendai virus)-AVE (artificial viral envelope), which is known for efficiency and reliability [16,20]. Instead of tail-vein injection, we chose direct injection into a lobe of the liver. This procedure has been demonstrated to be excellent in gene delivery and expression. When a complex of the HVJ-AVE liposome carrying a *lacZ* plasmid was injected directly into mouse liver, about 35% of the liver cells expressed beta-galactosidase [16].

Figure 2 shows two RNA/DNA chimeric oligonucleotides, LZ-2 and LZ-3, constructed to introduce a point mutation at the active site of LacZ. As in the successful studies, these oligonucleotides were prepared by ABI. The basic design of the chimeric oligonucleotides used here is the same as that in the previous studies [3,7,21]. They have 25 bp homology with the target, a GC clamp at the 3′ terminus and four T bases at the hairpins. The one strand of homologous region is comprised of 2′-*O*-methyl RNA that is thought to be important in initiating homologous pairing and stabilizing the structure [7,8]. The target sequence is 5′ GAA coding for Glu461 that is essential for the activity of LacZ [22,23]. LZ-2 is expected to change its 1st base (1436th base of the coding region) from G to C and generate a Glu461Gln mutation, which decreases activity 750-fold [23]. LZ-3 is expected to change its 2nd base (1437th base) from A to C and generate a Glu461Ala mutation, which decreases activity 120-fold [23]. The G to C change and the A to C change have been reported to be generated by the chimeric oligonucleotides [3,21,24,25]. The mutation in this target site (G1436A) was previously used to evaluate the efficiency of RNA/DNA oligonucleotides and single-stranded oligonucleotides for gene correction in cell culture and nuclear extracts [26–28]. This mutation is different from the mutations that LZ-2 or LZ-3 is predicted to introduce. We constructed the *lacZ*

mutant bacteriophage lambda strains and the strains were investigated with p-gal selection as follows.

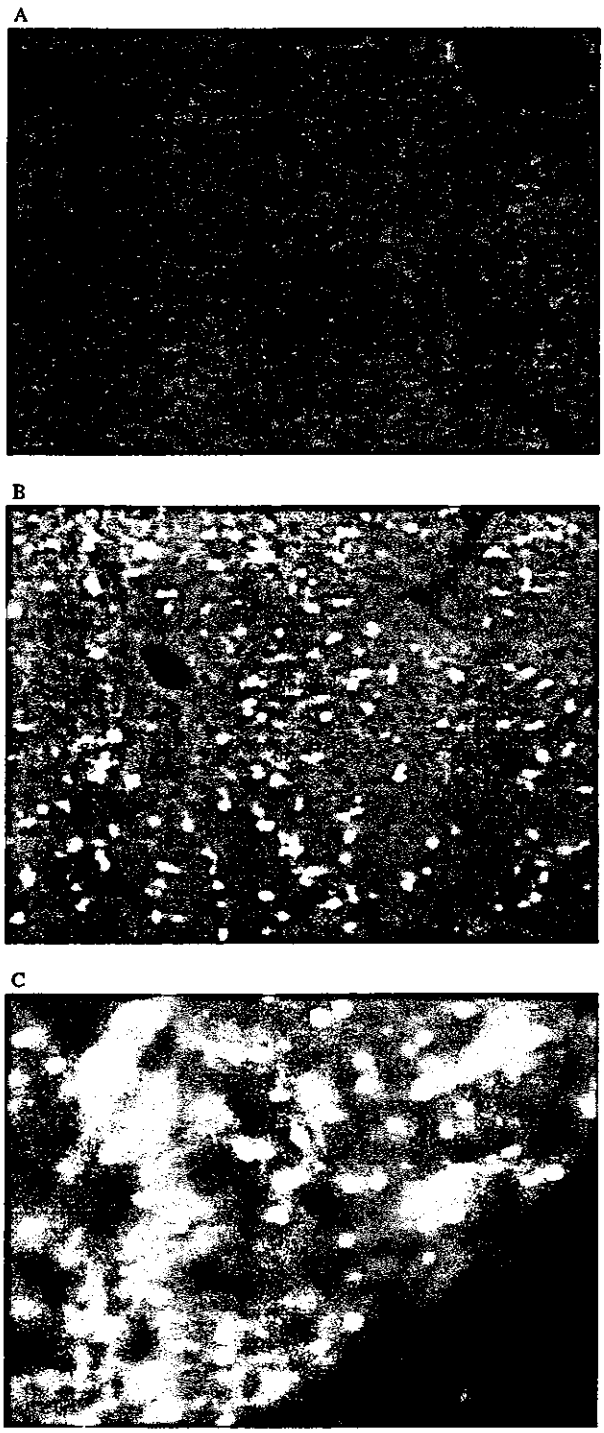

Figure 3. Transfer of FITC-labeled oligonucleotides to liver cells by direct injection with HVJ-AVE liposome. (A) Unlabeled oligonucleotides (×72). (B) FITC-labeled oligonucleotides (×72). (C) FITC-labeled oligonucleotides (×360). Unlabeled or FITC-labeled oligonucleotides were transfected to mouse liver by direct injection of HVJ-AVE liposome. The cells were observed under a fluorescence microscope 24 h later

Control experiments

We demonstrated that those *lacZ* mutants that are predicted to be generated by RNA/DNA oligonucleotides could be selected with p-gal as follows. We constructed the bacteriophage lambda strains carrying these mutations as detailed in Materials and methods. First, we subcloned the *lacZ* gene on a plasmid. Second, we introduced the expected mutations into this *lacZ* gene by site-directed mutagenesis. We sequenced the entire *lacZ* gene (1–3126) to show it has the single base-pair change. Third, we transferred this mutation back to lambda by homologous recombination *in vivo*.

The two lambda strains, lambda gt10 lacZ$^-$ Glu461Gln (LIA25) and lambda gt10 lacZ$^-$ Glu461Ala (LIA26), were used in the p-gal selection. As shown in Table 2, lambda with wild-type *lacZ* showed an efficiency of plaque formation less than 1/10 000 on the selective agar relative to that in non-selective agar. On the other hand, each of the mutant lambda strains showed an essentially identical efficiency of plaque formation in the selective agar and in the non-selective agar. We concluded that the targeted products of LZ-2 or LZ-3, if produced, should be selected with p-gal.

Delivery of FITC-labeled oligonucleotides with HVJ-AVE liposome

FITC-labeled oligonucleotides were introduced into mouse liver lobes by direct injection using the HVJ-AVE liposomes. Twenty-four hours later, the liver was removed, and its frozen sections were observed under a fluorescence microscope. The fluorescence was detected in every cell in the sample treated with the FITC-labeled oligonucleotides (Figure 3B), but not at all in the sample treated with the unlabeled oligonucleotides (Figure 3A). Strong fluorescence was detected in the nucleus in many of these cells: 286/1547 in the area for Figure 3B and 118/215 in the area for Figure 3C.

Gene delivery and measurement of mutant frequency

DNA was isolated from the treated liver and recovered as lambda phage particles by *in vitro* packaging. The *lacZ*-negative phages were selectively detected on agar with p-gal. The plaques on these selection plates were isolated,

Table 2. Selection efficiency of lambda *lacZ*-negative mutant

Lambda	Genotype	Titer	Titer on p-gal selective plate	Relative plaque formation efficiency
LIA22	*lacZ*$^+$	1.1×10^{10}	7.9×10^5	7.0×10^{-5}
LIA25	*lacZ*$^-$ Glu461Gln	5.0×10^7	4.6×10^7	9.4×10^{-1}
LIA26	*lacZ*$^-$ Glu461Ala	3.4×10^9	3.1×10^9	9.2×10^{-1}

Table 3. Detection of *lacZ*⁻ phage

	DNA/RNA chimera	Animal number	Total plaques	*lacZ*⁻ plaques	Mutant Frequency	Expected type
Exp. 1	None	1	4.8×10^4	7	15×10^{-5}	–
	LZ2	2	6.9×10^4	11	16×10^{-5}	0/11
	LZ2	3	6.5×10^4	9	14×10^{-5}	0/9
	LZ2	4	4.5×10^4	14	31×10^{-5}	0/14
Exp. 2	None	1	5.4×10^4	4	7×10^{-5}	–
	LZ3	5	5.4×10^4	1	2×10^{-5}	0/1
	LZ3	6	4.0×10^4	3	7×10^{-5}	0/3
	LZ3	7	2.6×10^4	1	4×10^{-5}	0/1

and the LacZ-negative phenotype was confirmed on agar plates with X-gal. The mutant frequency was estimated as the fraction of *lacZ*-negative phage (Table 3). The control mouse (animal number 1) was injected with phosphate-buffered saline (PBS) buffer/HVJ liposome lacking the RNA/DNA oligonucleotides. The mutant frequency of the injected mice was around the same level as this control mouse, which was approximately 1/10000 (Table 3). All the *lacZ*-negative phages were isolated and analyzed by way of sequencing or restriction. The *lacZ*-negative phages from the LZ-2-injected mice were analyzed for the sequence of the target region (1226–1466). However, the intended mutation was absent in any of the mutants. Their sequences were identical with the parental sequence. The *lacZ*-negative phages from LZ-3-injected mice were analyzed by restriction as illustrated in Figure 4A. A PCR product obtained from the predicted mutant DNA is not digested with TfiI. On the other hand, wild-type and the other mutants are digested with TfiI. All the *lacZ*-negative phages were digested with this restriction enzyme (Figure 4B). We did not detect the expected mutation in any of the isolates. In conclusion, gene correction frequency by these RNA/DNA oligonucleotides was shown to be less than 1/20000 in this system.

Discussion

The high efficiency gene correction with DNA/RNA chimeric oligonucleotides has been a subject of

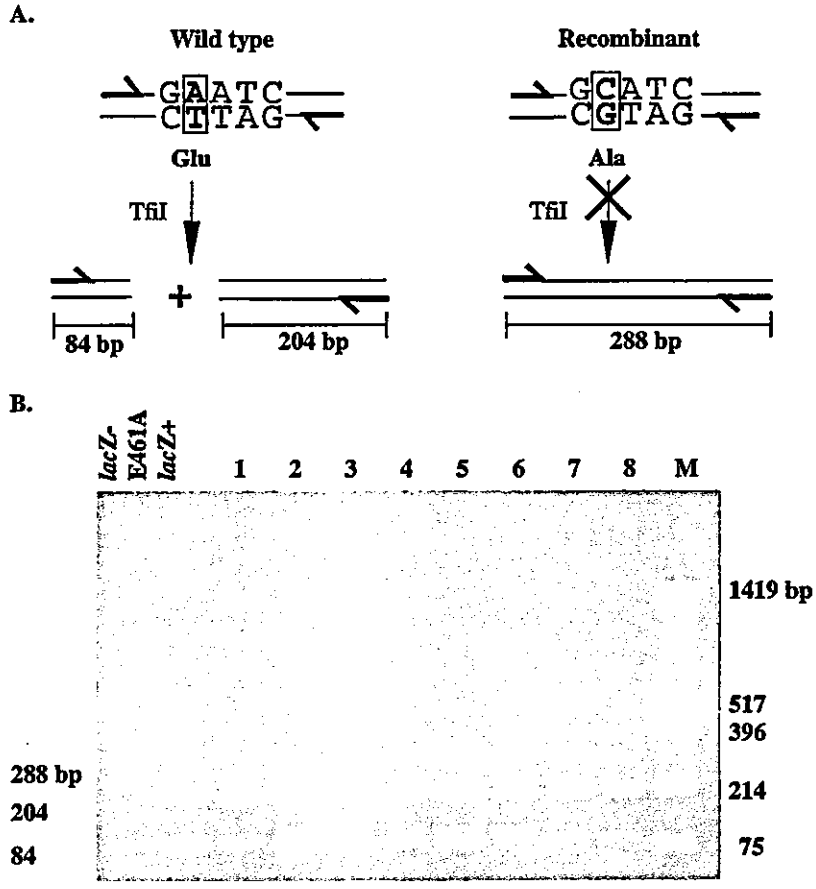

Figure 4. Restriction analysis of *lacZ*-negative phage from LZ-3 transferred mice. (A) The assay of PCR/restriction fragment length polymorphism for detection of Glu461Ala. The PCR product of lambda phage DNA using primers that flank the target site is 288 bp. The wild-type PCR product is digested with TfiI to 84 and 204 bp fragments, whereas the Glu461Ala mutant product is not. (B) Agarose gel electrophoresis of TfiI-digested PCR products. Lane M: Marker DNA prepared by HinfI digestion of plasmid pUC19; 1–3, *lacZ*-negative phage from animal number 7; 4–7, *lacZ*-negative phage from animal number 6; 8, *lacZ*-negative phage from animal number 5; *lacZ*⁺: Lambda phage recovered from control mouse; *lacZ*⁻ E461A: phage LIA26

controversy. We attempted to sensitively detect and quantitatively measure the efficiency of gene correction *in vivo* in a system that is free from the potential drawbacks of PCR-based assays used in the previous works. We chose a transgenic mouse system that allowed sensitive (1/10 000) detection of mutagenesis by various agents interacting with DNA in liver and other organs [14,29]. However, the designed mutations were not detected at all. The correction efficiency was shown to be less than 1/20 000 in the present system. We would like to discuss several factors that could be important for future success, for example, the delivery agents and target genomic sequences, and the quality of RNA/DNA oligonucleotides.

The HVJ-AVE liposome procedure we employed has been demonstrated to be efficient and reliable in gene delivery [20]. When the luciferase gene was injected directly into mouse liver, its expression was observed for at least 7 days [16]. Fluorescence was observed in essentially all the cells treated with FITC-labeled oligonucleotides (Figures 3B and 3C). Kawamura *et al.* reported that transfection of FITC-labeled oligonucleotides of either of three different sequences with the HVJ-liposome system showed a comparable efficiency as assessed by fluorescence [30]. Although the structures of FITC-labeled oligonucleotides and RNA/DNA chimeric oligonucleotides are different, we hypothesize that the RNA/DNA chimeric oligonucleotides were transfected at a comparable efficiency to FITC-labeled oligonucleotides.

When HVJ-liposome is introduced via tail-vein injection, the agent goes not only to liver, but also to kidney and spleen, and the efficiency is lower than in direct injection into liver [30]. That is why we chose direct injection. Our attempts at targeted gene correction by tail-vein injection of dsDNA-DMRIE-C (Gibco BRL) have been unsuccessful (N. Handa, Y. Naito and I. Kobayashi, unpublished results).

The effect of target sequences is difficult to evaluate. In the successful reports, GC contents of target sequences varies between 39.3% [5], 48.3% [4] and 60% [3]. On the other hand, in two failure reports, it was 76% [9,31]. GC contents of the target sequences of our LZ-2 and LZ-3 are 60% and 64%, respectively. Trying sites distant from the ones tried here might avoid any local effect and increase the likelihood of success.

The quality of RNA/DNA oligonucleotides is one of the most important factors reported [31]. The fraction of full-length oligonucleotides in the LZ-2 preparation and in the LZ-3 is 80% and 70%, respectively (Materials and methods). The fraction of oligonucleotides precisely with the designed sequence in these full-length oligonucleotides is estimated to be 36% from the average step-wise yield provided by ABI (98.5%). In electrophoresis using TBE (Tris-borate-EDTA)-urea polyacrylamide gel electrophoresis [31], LZ-2 gave a very sharp band, while LZ-3 gave a slightly fuzzier band (data not shown).

The MutaMouse has not been produced specifically to study gene correction. It contains 40 concatemeric copies of the *lacZ* shuttle vector rather than a single copy, mimicking an endogenous gene. If a specific mouse model were to be generated, the preferred option would be to introduce a single copy of mutated *lacZ* so that correction to the wild-type gene would result in a direct positive readout in the mouse body. Use of transgenic mice that could be generated from ES cells with a single copy of the mutant *lacZ* gene [28] would be ideal for this purpose. However, the presence of multiple copies might increase the sensitivity of detection. The use of only one mutation allele might limit the choice in mutation correction.

While this represents an *in vivo* study, it would be possible to carry out studies *in vitro* using skin fibroblasts or other sort of cell lines derived from MutaMouse (cf. a recent study in Gaucher's disease [12]), that would enable factors such as time, concentration and delivery vehicle to vary more easily. Such *in vitro* studies would provide a way to *in vivo* studies.

All we can say now is that the DNA/RNA chimeric oligonucleotide strategy for gene correction *in vivo* did not work in one system with one of the reliable gene delivery procedures and with one of the sensitive mutation detection procedures.

Acknowledgements

We thank Naofumi Handa and Yasuhiro Naito for permission to cite unpublished work, Dr. T. Suzuki for providing a bacterial strain, Dr. E. B. Kmiec for advice about handling RNA/DNA oligonucleotides, Drs. T. Nohmi and K. Masumura for advice about recovery of mouse DNA, and Dr. S. Tone for comments on the manuscript. This work was supported by grants from JOA (as arranged by Japan Society of Gene Therapy) and MEXT (Genome homeostasis).

References

1. Yanez RJ, Porter AC. Therapeutic gene targeting. *Gene Ther* 1998; 5: 149–159.
2. Capecchi MR. Altering the genome by homologous recombination. *Science* 1989; 244: 1288–1292.
3. Kren BT, Bandyopadhyay P, Steer CJ. In vivo site-directed mutagenesis of the factor IX gene by chimeric RNA/DNA oligonucleotides. *Nat Med* 1998; 4: 285–290.
4. Kren BT, Parashar B, Bandyopadhyay P, *et al.* Correction of the UDP-glucuronosyltransferase gene defect in the gunn rat model of crigler-najjar syndrome type I with a chimeric oligonucleotide. *Proc Natl Acad Sci U S A* 1999; 96: 10 349–10 354.
5. Rando TA, Disatnik MH, Zhou LZ. Rescue of dystrophin expression in mdx mouse muscle by RNA/DNA oligonucleotides. *Proc Natl Acad Sci U S A* 2000; 97: 5363–5368.
6. Beetham PR, Kipp PB, Sawycky XL, *et al.* A tool for functional plant genomics: chimeric RNA/DNA oligonucleotides cause in vivo gene-specific mutations. *Proc Natl Acad Sci U S A* 1999; 96: 8774–8778.
7. Yoon K, Cole-Strauss A, Kmiec EB. Targeted gene correction of episomal DNA in mammalian cells mediated by a chimeric RNA.DNA oligonucleotide. *Proc Natl Acad Sci U S A* 1996; 93: 2071–2076.
8. Gamper HB Jr, Cole-Strauss A, Metz R, *et al.* A plausible mechanism for gene correction by chimeric oligonucleotides. *Biochemistry* 2000; 39: 5808–5816.
9. Thorpe PH, Stevenson BJ, Porteous DJ. Functional correction of episomal mutations with short DNA fragments and RNA-DNA oligonucleotides. *J Gene Med* 2002; 4: 195–204.
10. van der Steege G, Schullenga-Hut PH, Buys CH, *et al.* Persistent failures in gene repair. *Nat Biotechnol* 2001; 19: 305–306.

11. Taubes G. Gene therapy. The strange case of chimeraplasty. *Science* 2002; 298: 2116–2120.
12. Diaz-Font A, Cormand B, Chabas A, *et al.* Unsuccessful chimeraplast strategy for the correction of a mutation causing Gaucher disease. *Blood Cells Mol Dis* 2003; 31: 183–186.
13. Gossen JA, de Leeuw WJ, Tan CH, *et al.* Efficient rescue of integrated shuttle vectors from transgenic mice: a model for studying mutations *in vivo*. *Proc Natl Acad Sci U S A* 1989; 86: 7971–7975.
14. Cosentino L, Heddle JA. A comparison of the effects of diverse mutagens at the lacZ transgene and Dlb-1 locus in vivo. *Mutagenesis* 1999; 14: 113–119.
15. Myhr BC. Validation studies with Muta Mouse: a transgenic mouse model for detecting mutations in vivo. *Environ Mol Mutagen* 1991; 18: 308–315.
16. Saeki Y, Wataya-Kaneda M, Tanaka K, *et al.* Sustained transgene expression *in vitro* and *in vivo* using an Epstein-Barr virus replicon vector system combined with HVJ liposomes. *Gene Ther* 1998; 5: 1031–1037.
17. Dean SW, Myhr B. Measurement of gene mutation *in vivo* using Muta Mouse and positive selection for *lacZ*$^-$ phage. *Mutagenesis* 1994; 9: 183–185.
18. Gossen JA, Vijg J. A selective system for *lacZ*$^-$ phage using a galactose-sensitive *E. coli* host. *Biotechniques* 1993; 14: 326–330.
19. Blakey DH, Douglas GR, Huang KC, *et al.* Cytogenetic mapping of lambda gt10 *lacZ* sequences in the transgenic mouse strain 40.6 (Muta Mouse). *Mutagenesis* 1995; 10: 145–148.
20. Saeki Y, Matsumoto N, Nakano Y, *et al.* Development and characterization of cationic liposomes conjugated with HVJ (Sendai virus): reciprocal effect of cationic lipid for *in vitro* and *in vivo* gene transfer. *Hum Gene Ther* 1997; 8: 2133–2141.
21. Bandyopadhyay P, Ma X, Linehan-Stieers C, *et al.* Nucleotide exchange in genomic DNA of rat hepatocytes using RNA/DNA oligonucleotides. Targeted delivery of liposomes and polyethyleneimine to the asialoglycoprotein receptor. *J Biol Chem* 1999; 274: 10163–10172.
22. Jacobson RH, Zhang XJ, DuBose RF, *et al.* Three-dimensional structure of beta-galactosidase from *E. coli*. *Nature* 1994; 369: 761–766.
23. Cupples CG, Miller JH. Effects of amino acid substitutions at the active site in *Escherichia coli* beta-galactosidase. *Genetics* 1988; 120: 637–644.
24. Cole-Strauss A, Gamper H, Holloman WK, *et al.* Targeted gene repair directed by the chimeric RNA/DNA oligonucleotide in a mammalian cell-free extract. *Nucleic Acids Res* 1999; 27: 1323–1330.
25. Chen Z, Felsheim R, Wong P, *et al.* Mitochondria isolated from liver contain the essential factors required for RNA/DNA oligonucleotide-targeted gene repair. *Biochem Biophys Res Commun* 2001; 285: 188–194.
26. Nickerson HD, Colledge WH. A comparison of gene repair strategies in cell culture using a lacZ reporter system. *Gene Ther* 2003; 10: 1584–1591.
27. Igoucheva O, Alexeev V, Pryce M, *et al.* Transcription affects formation and processing of intermediates in oligonucleotide-mediated gene alteration. *Nucleic Acids Res* 2003; 31: 2659–2670.
28. Pierce EA, Liu Q, Igoucheva O, *et al.* Oligonucleotide-directed single-base DNA alterations in mouse embryonic stem cells. *Gene Ther* 2003; 10: 24–33.
29. Krebs O, Favor J. Somatic and germ cell mutagenesis in lambda lacZ transgenic mice treated with acrylamide or ethylnitrosourea. *Mutat Res* 1997; 388: 239–248.
30. Kawamura I, Morishita R, Tsujimoto S, *et al.* Intravenous injection of oligodeoxynucleotides to the NF-kappaB binding site inhibits hepatic metastasis of M5076 reticulosarcoma in mice. *Gene Ther* 2001; 8: 905–912.
31. Manzano A, Mohri Z, Sperber G, *et al.* Failure to generate atheroprotective apolipoprotein AI phenotypes using synthetic RNA/DNA oligonucleotides (chimeraplasts). *J Gene Med* 2003; 5: 795–802.

Enhanced Tumor-Specific Long-Term Immunity of Hemagglutinating Virus of Japan-Mediated Dendritic Cell-Tumor Fused Cell Vaccination by Coadministration with CpG Oligodeoxynucleotides[1]

Kazuya Hiraoka,*† Seiji Yamamoto,* Satoru Otsuru,* Seiji Nakai,* Katsuto Tamai,* Ryuichi Morishita,‡ Toshio Ogihara,† and Yasufumi Kaneda[2]*

Immunization with dendritic cells (DCs) using various Ag-loading approaches has shown promising results in tumor-specific immunotherapy and immunoprevention. Fused cells (FCs) that are generated from DCs and tumor cells are one of effective cancer vaccines because both known and unknown tumor Ags are presented on the FCs and recognized by T cells. In this study, we attempted to augment antitumor immunity by the combination of DC-tumor FC vaccination with immunostimulatory oligodeoxynucleotides containing CpG motif (CpG ODN). Murine DCs were fused with syngeneic tumor cells ex vivo using inactivated hemagglutinating virus of Japan (Sendai virus). Mice were intradermally (i.d.) immunized with FCs and/or CpG ODN. Coadministration of CpG ODN enhanced the phenotypical maturation of FCs and unfused DCs, and the production of Th1 cytokines, such as IFN-γ and IL-12, leading to the induction of tumor-specific CTLs without falling into T cell anergy. In addition, immunization with FCs + CpG ODN provided significant protection against lethal s.c. tumor challenge and spontaneous lung metastasis compared with that with either FCs or CpG ODN alone. Furthermore, among mice that rejected tumor challenge, the mice immunized with FCs + CpG ODN, but not the mice immunized with FCs or CpG ODN alone, completely rejected tumor rechallenge, indicating that CpG ODN provided long-term maintenance of tumor-specific immunity induced by FCs. Thus, the combination of DC-tumor FCs and CpG ODN is an effective and feasible cancer vaccine to prevent the generation and recurrence of cancers. *The Journal of Immunology,* **2004, 173: 4297–4307.**

Although surgery, chemotherapy, and radiotherapy are effective cancer treatments, some cancers are refractory to these treatments. Effective treatment of advanced and metastatic cancers and the prevention of recurrence are especially difficult. Immunotherapy and immunoprevention are promising approaches to cancer treatment and prevention that may someday overcome the shortcomings of traditional cancer managements.

Two different signals are required to prime and activate naive $CD4^+$ and $CD8^+$ T cells (1). First, antigenic peptides must be presented on the surface of activated APCs by MHC class I or II molecules to $CD8^+$ or $CD4^+$ T cells, respectively. The binding of peptide/MHC complexes to TCRs mediates a signal into the T cells. A second signal must be mediated from costimulatory molecules on activated APCs to T cells. Thus, it is essential for cancer vaccines to activate APCs, such as dendritic cells (DCs),[3] that can recognize and present tumor Ags to T cells (2).

Tumor-associated Ags (TAAs) presented by mature DCs are needed to evoke tumor-specific immune response. Several melanoma Ags recognized by T cells have been identified, including MAGE, gp100, MART-1, TRP-1, TRP-2, and tyrosinase (3). DCs treated with TAA peptides or tumor lysates enhanced tumor immunity in melanoma patients (4). TAAs have also been identified in cancers other than melanoma (5). However, TAAs in many cancers have not been identified.

To solve this problem, hybrid cell vaccines have been developed by fusing mature DCs with tumor cells. DC-tumor fused cells (FCs) express known and unknown TAAs, as well as high levels of MHC class I and II molecules and costimulatory molecules that can prime and activate naive $CD4^+$ and $CD8^+$ T cells (6). Therefore, even though tumor cells lose the expression of MHC class I molecules, TAAs can be presented on the surface of FCs by DC-derived MHC class I molecules.

It has been reported that vaccinations of mice with DC-tumor FCs induce therapeutic and protective immune responses against established and spontaneous tumors, which included both immunogenic and poorly immunogenic tumors (7–12). In these studies, FCs were generated by polyethylene glycol (PEG) (7–10) or electrofusion (11, 12). In vitro studies using human cells have shown that DC-tumor FCs present both known and unknown TAAs in the context of HLA class I molecules and induce tumor-specific CTL response (10). In clinical trials, patients with malignant glioma (13) or melanoma (14) were vaccinated with autologous DC-tumor

*Division of Gene Therapy Science, †Department of Geriatric Medicine, and ‡Division of Clinical Gene Therapy, Graduate School of Medicine, Osaka University, Suita, Osaka, Japan

Received for publication March 11, 2004. Accepted for publication July 22, 2004.

The costs of publication of this article were defrayed in part by the payment of page charges. This article must therefore be hereby marked *advertisement* in accordance with 18 U.S.C. Section 1734 solely to indicate this fact.

[1] This work was supported by Grant 13218069 from the Ministry of Education, Culture, Sports, Science and Technology of Japan.

[2] Address correspondence and reprint requests to Dr. Yasufumi Kaneda, Division of Gene Therapy Science, Graduate School of Medicine, Osaka University, 2-2 Yamadaoka, Suita, Osaka 565-0871, Japan. E-mail address: kaneday@gts.med.osaka-u.ac.jp

[3] Abbreviations used in this paper: DC, dendritic cell; TAA, tumor-associated Ag; FC, fused cell; CpG ODN, oligodeoxynucleotides containing CpG motif; HVJ, hemagglutinating virus of Japan; HAU, hemagglutinating units; BSS, balanced salt solution; i.d., intradermal(ly); PEG, polyethylene glycol.

0022-1767/04/$02.00

FCs generated by PEG. These vaccinations were safe, but only induced weak clinical responses.

TAA alone is not sufficient for producing effective vaccines, and the aid of adjuvants to enhance vaccine effects has been pointed out (15). Adjuvants play an important role in determining the quality and quantity of immune response to Ags. Many adjuvants including recombinant Th1 cytokines, such as IL-2 and IL-12, as well as Freund's adjuvant, aluminum salts, and monophosphoryl lipid have been used in animals and humans (16). However, these adjuvants resulted in little or no immune enhancement and caused toxicity in some cases.

Recently, synthetic oligodeoxynucleotides containing specific bacterial unmethylated CpG motif (CpG ODN), which are one of so-called pathogen-associated molecular patterns, have attracted a great deal of attention as a novel and safe adjuvant (17–19). CpG ODN are recognized by cells of innate immune system of vertebrates, such as B cells, macrophages, monocytes, and DCs, and activate these cells (17, 18). CpG ODN preferentially induce Th1 immune response through its receptor, TLR9, with the production of cytokines, such as TNF-α, IL-12, and IFN-γ, appropriate for the development of antitumor immunity (20). Indeed, the use of CpG ODN as an adjuvant combined with other immunotherapies, such as TAA peptide-pulsed DCs (21), or as a monotherapy (22) induced antitumor response in mice, while TAA peptide-pulsed DCs alone were not effective. The effect of CpG ODN on human cancers is currently being evaluated in clinical trials (23).

Several studies of DC-tumor FC vaccines in mice have reported that coadministration of FCs with rIL-2 (8) or IL-12 (9, 11) by i.p. injection as an adjuvant enhances the antitumor effect more effectively compared with that induced by either FCs or the adjuvant alone. These results suggest the need of adjuvant to enhance antitumor immunity in the use of FCs for cancer vaccines.

In this study, we investigated whether CpG ODN could safely enhance tumor-specific immune response induced by DC-tumor FC vaccines generated by inactivated hemagglutinating virus of Japan (HVJ; Sendai virus).

Materials and Methods

Materials

All cell lines, including B16BL6 melanoma (H-2^b), EL4 T cell lymphoma (H-2^b), RENCA renal cell carcinoma (H-2^d), and CT26 colon adenocarcinoma (H-2^d), were purchased from American Type Culture Collection (Manassas, VA). Synthesized ODN, such as phosphorothioate-modified CpG ODN (CpG 1668; 5′-TCCAT GACGTTCCTGATGCT-3′) and non-CpG ODN (GpG 1668; 5′-TCCATGAGGTTCCTGATGCT-3′) (18), were purchased from Hokkaido System Science (Sapporo, Japan). Male 8-wk-old C57BL/6 (H-2^b) and BALB/c (H-2^d) mice were purchased from Oriental Yeast (Tokyo, Japan) and maintained in a temperature-controlled, pathogen-free room. All animals were handled according to approved protocols and the guidelines of the Animal Committee of Osaka University.

Preparation and culture of DCs

Murine bone marrow-derived DCs were generated as previously described (24) with minor modifications (25). Briefly, after flushing out bone marrow of tibia and femur with RPMI 1640 medium, effluent tissue was passed through 40-μm mesh, and erythrocytes were lysed with ammonium chloride. After washing, 1×10^6 cells were plated in 24-well plates (Costar, Corning, NY) in 1 ml of RPMI 1640 medium supplemented with 10% heat-inactivated FBS (Equitech-Bio, Kerrville, TX), antibiotics, 50 μM 2-ME, and 10 ng/ml recombinant murine GM-CSF (Genzyme-Techne, Minneapolis, MN). The cultures were fed every other day by gentle pipetting, aspirating all of the medium, and adding fresh medium. On day 6 of culture, nonadherent and loosely adherent clusters of proliferating DCs were collected, and 1×10^6 cells were replated in 24-well plates in 1 ml of DC medium with 100 ng/ml LPS (*Escherichia coli* 055:B5) (Sigma-Aldrich, St. Louis, MO) for 24 h. On day 7 of culture, nonadherent DCs were harvested and used for fusion. More than 90% of these DCs were positive for CD11c and displayed a typical mature phenotype as confirmed by flow cytometry.

HVJ-mediated cell fusion

HVJ (Z strain) was purified from chorioallantoic fluid of chick eggs by centrifugation, and the titer was calculated as previously described (26). The virus was inactivated by UV irradiation (99 mJ/cm^2) just before use. With this preparation, the ability of virus replication was lost completely, but fusion activity was not affected as previously described (27). To determine optimal fusion efficiency, mature DCs and tumor cells were labeled with fluorescent red and green, respectively, using PKH26 and PKH67 according to the manufacturer's instructions (Zynaxis Cell Science, Malvern, PA). PKH dyes were intensively washed to remove the unbound dyes and to avoid leakage of the bound dyes between DCs and tumor cells. Alternatively, mature DCs and B16BL6 cells were labeled with FITC-conjugated anti-mouse mAb against CD11c and anti-human gp100 primary mAb (DakoCytomation, Glostrup, Denmark) followed by PE-conjugated anti-mouse κ L chain secondary mAb (BD Pharmingen, San Diego, CA), respectively. FITC mAbs against CD40, CD80, CD86, or MHC class II were also used as DC markers. The tumor cells were then irradiated with 100 Gy using ^{137}Cs gamma rays generated by Gammacell (MDS Nordion, Ottawa, Ontario, Canada) and fused with mature DCs at a ratio of 1:2 using HVJ as previously described (28) with some modifications. Briefly, mature DCs (4×10^6 cells) suspended in 250 μl of balanced salt solution (BSS; 10 mM Tris-Cl (pH 7.5), 137 mM NaCl, 5.4 mM KCl) containing 2 mM $CaCl_2$ and irradiated tumor cells (2×10^6 cells) suspended in 250 μl of BSS containing 2 mM $CaCl_2$ and various amounts of HVJ (0–1000 hemagglutinating units (HAU)) suspended in 500 μl of BSS were mixed in a 2-ml tube. After incubation at 0°C for 5 min, the mixture was incubated at 37°C for 15 min with shaking (120 rpm) in a water bath to induce cell-cell fusion. After centrifugation at 1200 rpm for 3 min at 4°C, the fusion products were washed twice with 1.5 ml of BSS to remove the free HVJ and cultured overnight at 37°C in 5% CO_2. After 24-h culture following fusion, the fusion products were harvested. Fusion efficiency was evaluated with FACScan and FACSVantage (BD Biosciences, San Jose, CA). FCs collected using FACSVantage (BD Biosciences) were subjected to some experiments.

Phenotypic analysis

After fusion between nonlabeled mature DCs and PKH26-labeled B16BL6 cells using 500 HAU of inactivated HVJ, the fusion products were cultured for 24 h with or without 10 μg/ml CpG ODN, followed by staining with FITC mAbs against CD11c, CD40, CD80, CD86, or MHC class II as DC markers. Surface phenotypes of FCs were analyzed by gating and excluding single red-positive cells using FACSVantage (BD Biosciences).

Immunization in vivo

After 12-h incubation of fusion products generated from DCs and irradiated syngeneic tumor cells (B16BL6 or RENCA cells) using 0 HAU (i.e., Mix) or 500 HAU (i.e., FCs) of HVJ, 6×10^6 cells were harvested and suspended in 200 μl of PBS. CpG ODN (100

μg) was dissolved in 100 μl of PBS and mixed with 100 μl of PBS (i.e., CpG alone) or 6×10^6 cells suspended in 100 μl of PBS (i.e., Mix + CpG and FCs + CpG) immediately before injection into mice. In some experiments, FCs were collected with a cell sorter, and 1.2×10^6 FCs (i.e., sorted FCs) were injected into mice. The mice (10 mice/group) were immunized twice, at weekly intervals as reported previously (9, 29, 30), with one of these vaccination protocols in a total volume of 200 μl of PBS by i.d. injection into the bilateral posterior flanks near the base of the tail (100 μl per flank). We selected this route of immunization because FCs migrate into draining lymph nodes after i.d. injection (31, 32). The number of cells in the fusion products was described based on the number of cells that were used in the DC-tumor cell fusion.

Cytokine measurements

After 24-h incubation of fusion products generated by 0 HAU (i.e., Mix) or 500 HAU (i.e., FCs) of HVJ with or without 10 μg/ml CpG ODN, the supernatants were harvested before immunization and stored at −80°C. After in vivo immunization, cell culture supernatants of isolated spleen cells on day 5 during restimulation were also collected and stored at −80°C. The concentrations of TNF-α, IL-12 p40, IFN-γ, and IL-4 in the supernatants were measured by ELISA Development kits (Genzyme-Techne).

Cytolytic assay

Ten days after the second immunization, spleen cells were pooled from each group of mice (three mice per group). The spleen cells (5×10^6 cells/well) were cocultured to restimulate with mitomycin C-treated tumor cells at a ratio of 20:1 in 2 ml of T cell culture medium (RPMI 1640 medium supplemented with 10% heat-inactivated FBS, antibiotics, and 50 μM 2-ME) in 24-well plates at 37°C in 5% CO_2. The cells, which contained CTLs, were harvested on day 5 and used as effector cells in a standard 4-h ^{51}Cr release assay to examine antitumor cytolytic activity. Briefly, target tumor cells (1×10^6) were labeled with 100 μCi of $Na_2{}^{51}CrO_4$ (Amersham Biosciences, Buckinghamshire, U.K.) in 200 μl of RPMI 1640 supplemented with 10% heat-inactivated FBS for 90 min at 37°C. The labeled target cells (1×10^4 cells/well) were incubated with the effector cells for 4 h at 37°C in 96-well microtiter plates in 200 μl of T cell medium at various E:T ratios. The plates were then centrifuged, and the radioactivity of the supernatants was counted using a MicroBeta Trilux Scintillation Counter (Wallac, Gaithersburg, MD). The maximum or spontaneous release was defined as counts from samples incubated with 2% Triton X-100 or medium alone, respectively. Cytolytic activity was calculated using the following formula: percentage of specific ^{51}Cr release = (experimental release − spontaneous release) × 100/(maximum release − spontaneous release). Assays were performed in triplicate wells. The spontaneous release in all assays was <20% of the maximum release.

Prophylactic treatment in s.c. tumor model

Ten days after the second vaccination, C57BL/6 mice were challenged by s.c. injection with 1×10^5 B16BL6 cells, and BALB/c mice were injected s.c. with 1×10^5 RENCA cells into the back different, but proximal, from two vaccinated sites. After tumor challenge, mice were monitored daily. Tumor incidence was considered positive when the tumor length exceeded 3 mm. Tumor size was measured every other day in a blinded manner with digital calipers. Tumor volume was calculated using the following formula: tumor volume (mm^3) = length × $(\text{width})^2/2$ (Ref. 33). Mice were euthanized when tumors became ulcerated or surpassed 4000 mm^3 in volume. Sixty days after tumor inoculation, tumor-free C57BL/6 or BALB/c mice were rechallenged s.c. with 1×10^5 B16BL6 cells and 5×10^4 EL4 cells or 1×10^5 RENCA cells and 5×10^4 CT26 cells, respectively, injected into the back to clarify tumor specificity of the vaccination in vivo.

Prophylactic treatment in spontaneous lung metastasis model

B16BL6 melanoma cells are highly invasive and spontaneously metastatic from the primary site (34). Ten days after the second vaccination, C57BL/6 mice (eight mice per group) were injected s.c. with 5×10^5 B16BL6 cells suspended in 50 μl of PBS into the right hind footpad to initiate primary tumor growth. On day 21 after tumor inoculation, when the primary tumor was >10 mm in length, it was surgically removed by a right hip disarticulation with removal of the regional draining popliteal and inguinal lymph nodes. All mice were euthanized 21 days after surgery, and the lungs were fixed in Bouin's solution (Sigma-Aldrich). The number of lung metastases was counted under a dissecting microscope (35).

Statistical analysis

Statistical analysis was performed with StatView software (Abacus Concepts, Berkeley, CA). The χ^2 test was used to analyze differences between percentages of tumor-free mice at day 60. The log-rank test was used to analyze Kaplan-Meier survival curves. The unpaired Fisher's protected least significant difference test was used in other analyses. We defined statistical significance as $p < 0.05$.

Results

HVJ-mediated DC-tumor cell fusion

We used inactivated HVJ to generate DC-tumor FCs. Murine DCs (4×10^6 cells) stained with PKH26 (shown in red) and irradiated B16BL6 cells (2×10^6 cells) stained with PKH67 (shown in green) were fused with UV-inactivated HVJ. After 24-h incubation, the fusion products were analyzed by flow cytometry. Fluorescent microscopic observation after sorting each fraction revealed that double-positive cells in the *upper right* fraction were large and fluorescent yellow DC-tumor FCs, while the *lower right* and *upper left* fractions contained unfused B16BL6 cells and DCs, respectively (Fig. 1*A*).

To determine the optimal fusion conditions, fusion efficiency and cell viability of fusion products generated by various amounts of HVJ (0–1000 HAU) were investigated. Fusion efficiency analyzed by flow cytometry was 5.38, 13.71, 25.49, and 26.57% with 0, 100, 500, and 1000 HAU of inactivated HVJ, respectively (Fig. 1*B*). Spontaneous double-positive cells were obtained at low efficiency (5.38%) even in the absence of HVJ, maybe resulting from the capture of irradiated tumor cells by DCs (Fig. 1*B*, 0 HAU). Cell viability assessed by lactose dehydrogenase release assay was 96, 93, 85, and 60% after 24-h culture following fusion, and 74, 67, 60, and 25% after 72-h culture following fusion with 0, 100, 500, and 1000 HAU, respectively (500 HAU vs 1000 HAU, $p < 0.05$). We obtained similar results for fusion efficiency and cell viability in at least 10 separate experiments. Therefore, we chose 500 HAU of inactivated HVJ to generate DC-tumor FCs in the following experiments.

Furthermore, we analyzed the expression of specific markers derived from DCs and B16BL6 melanoma cells in DC-tumor FCs. FACS analysis (Fig. 2*A*) showed that, with 500 HAU of inactivated HVJ, cells expressing both DC surface markers such as CD11c, CD40, CD80, CD86, or MHC class II and B16BL6 marker, gp100, were generated at ~30% efficiency. Without HVJ (indicated as 0 HAU in Fig. 2*A*), cells with both surface markers were 3–9% in this assay. Fluorescent microscopic observation of the fusion products generated from DCs stained with FITC mAb against CD11c (Fig. 2*B*, *left panel*), a DC marker, and B16BL6

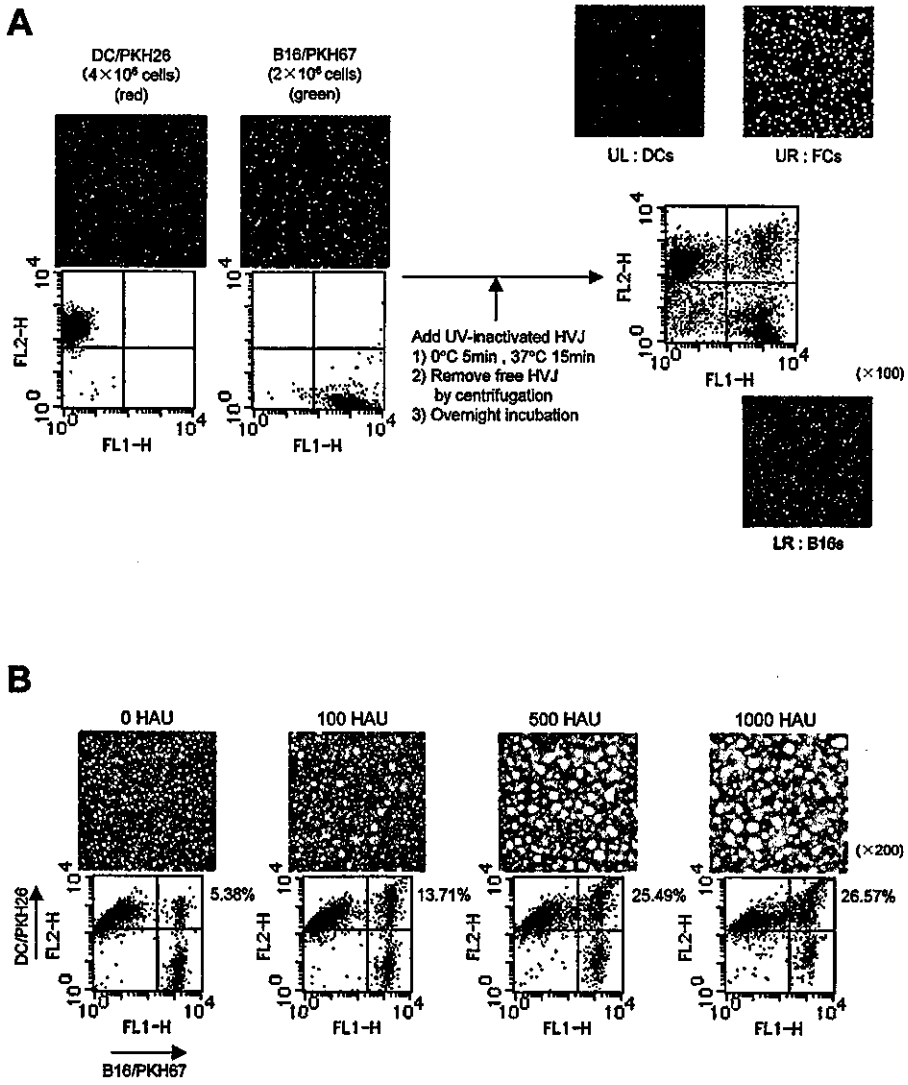

FIGURE 1. HVJ-mediated DC-tumor cell fusion. *A*, Fusion protocol. Bone marrow-derived DCs (4×10^6 cells) stained with PKH26 (red) and irradiated B16BL6 cells (2×10^6 cells) stained with PKH67 (shown in green) were mixed at a 2:1 ratio, and fused with UV-inactivated HVJ. The free HVJ was removed by centrifugation and washing with BSS, and the cells were cultured at 37°C in 5% CO_2. After 24-h incubation, the fusion products were collected. Double-positive (*upper right*), single green-positive (*lower right*), and single red-positive cells (*upper left*) were sorted using flow cytometry and observed by fluorescent microscopy (magnification, ×100). *B*, Fusion efficiency. Various amounts of HVJ (0–1000 HAU) were used to fuse DCs stained with PH26 (shown in red) and irradiated B16BL6 cells stained with PKH67 (shown in green). The fusion efficiency was assessed by flow cytometry. Fluorescence microscopy was used to demonstrate DC-B16BL6 FCs, shown as large yellow cells (magnification, ×200).

cells stained with PE mAb against gp100 TAA (Fig. 2*B*, *center panel*), a B16BL6 cell marker, showed that DC-B16BL6 FCs were positive for both markers (Fig. 2*B*, *right panel*). These findings indicate that inactivated HVJ could be used as a fusogen for DC-tumor cell fusion.

Enhanced phenotypical maturation and Th1 cytokine production of FCs by administration with CpG ODN in vitro

We analyzed the phenotypical maturation of FCs containing unfused DCs by examining the expression of various surface markers of DCs. The expression of surface markers of DCs was up-regulated by the treatment with 100 ng/ml LPS, and maintained in FCs after fusion (Fig. 3*A*). The phenotypical maturation of FCs was further enhanced by 10 μg/ml CpG ODN, especially in CD80, CD86, and MHC class II (Fig. 3*A*). We also analyzed the production of Th1 cytokines, such as TNF-α and IL-12, from the mixture of mature DCs and B16BL6 cells (Mix) or FCs. FCs produced significantly more TNF-α than Mix (Fig. 3*B*). The production of IL-12 p40 was comparable between FCs and Mix (Fig. 3*C*). The amount of both cytokines produced by FCs or Mix was approximately doubled when CpG ODN were administered with the cells. However, non-CpG ODN did not enhance the production of these cytokines (Fig. 3, *B* and *C*). The highest production of these cytokines was obtained in the supernatants of FCs incubated with 10 μg/ml CpG ODN (FCs + CpG). CpG ODN did not affect the viability of FCs (data not shown). We also found that mature DCs treated with inactivated HVJ did not enhance the cytokine production (data not shown). These results indicate that CpG ODN, but not inactivated HVJ, could promote further phenotypical maturation and activation of FCs.

Enhanced tumor-specific immune response of FCs by coadministration with CpG ODN in vivo

To assess whether tumor-specific CTLs were induced after immunization with FCs, two parameters of effector function, IFN-γ and IL-4 production and cytolytic activity, were investigated (Fig. 4). IFN-γ secreted from spleen cells on day 5 during restimulation with B16BL6 cells was highest when the mice were vaccinated with the combination of FCs and CpG ODN (FCs + CpG; Fig. 4*A*). To examine cytokine production from only FCs, we sorted DC-tumor hybrid cells using a cell sorter. IFN-γ production in sorted FCs was similar to that in FCs in the absence of CpG ODN. Furthermore, the production of IFN-γ in sorted FCs was enhanced with CpG ODN as much as that in FCs. Although the production of Th2 cytokine, IL-4, was also enhanced with either FCs or sorted FCs, the amount was much less than IFN-γ.

Cytolytic activity of spleen cells from the mice immunized with FCs was significantly higher compared with that from other vaccination protocols, such as PBS, CpG, Mix, and Mix + CpG (Fig. 4*B*). Furthermore, the highest cytolytic activity was observed in

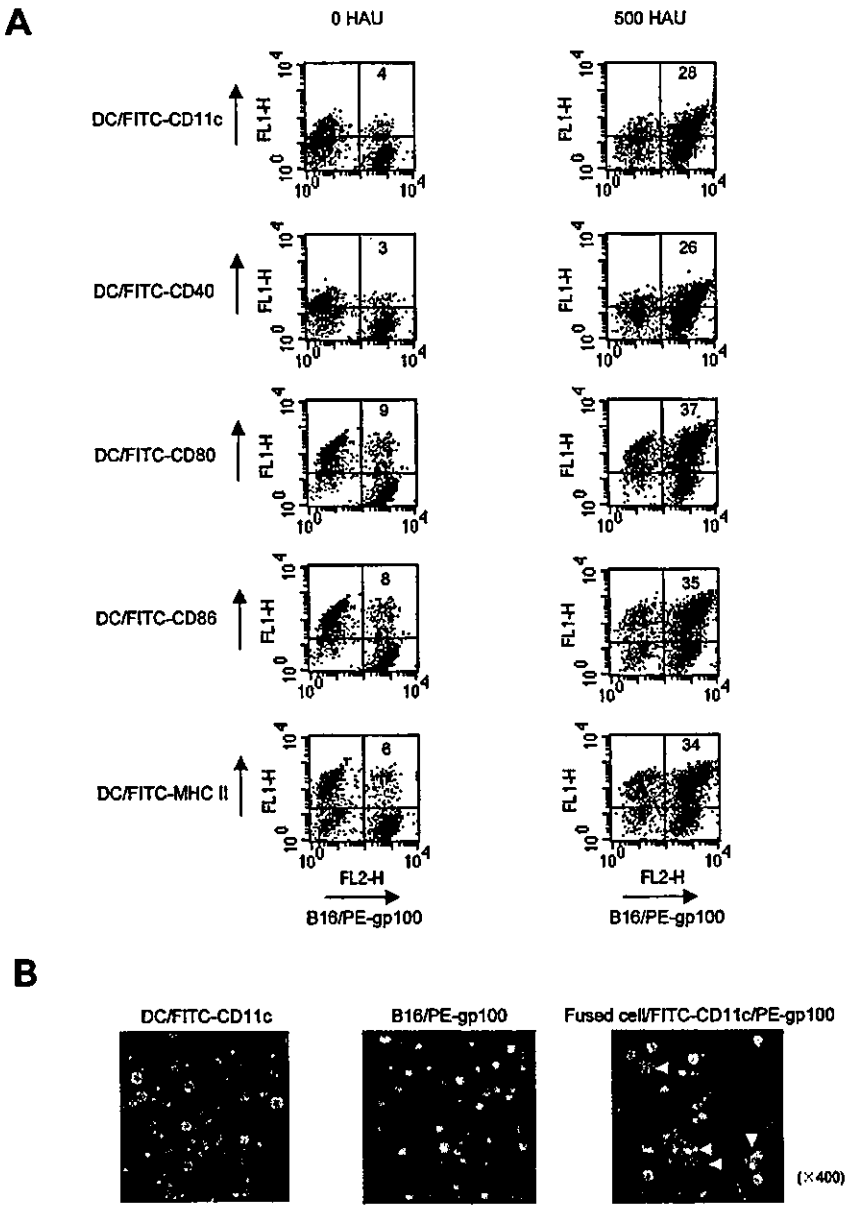

FIGURE 2. Characterization of DC-tumor FCs. *A*, FACS analysis of DC-tumor FCs generated by inactivated HVJ. After 24-h incubation of fusion products with (500 HAU) or without (0 HAU) inactivated HVJ, surface phenotypes of DCs and gp100 expression of B16BL6 were analyzed by flow cytometry. Each number indicates the percentage of double-positive cells. These experiments were repeated twice with similar results. *B*, Identification of DC-tumor FCs with specific markers. After 24-h culture of fusion products generated from DCs, stained with FITC mAb against CD11c (*left*) as a DC marker, and B16BL6 cells, stained with PE mAb against gp100 TAA (*center*) as a B16BL6 cell marker, fluorescent microscopy showed that DC-B16BL6 FCs were double-positive cells expressing both markers (*right*) with ~20% fusion efficiency. White arrows indicate DC-B16BL6 FCs (magnification, ×400).

the mice that received FCs + CpG compared with that in the mice that received FCs alone (Fig. 4*B*). No cytolytic effect was observed when other syngeneic tumor cells, EL4 T cell lymphoma cells, were used as the target cells (Fig. 4*C*). These results indicate that CpG ODN strongly enhanced the tumor-specific immune response generated by FCs.

Enhanced prophylactic effect of FCs coadministered with CpG ODN on the growth of mouse tumors

The effect of vaccination with FCs + CpG on the inhibition of s.c. tumor growth was investigated in a melanoma model (Fig. 5). After the challenge with 1×10^5 B16BL6 cells, mice immunized with FCs + CpG significantly inhibited tumor growth compared with mice that received either FCs or CpG ODN alone (Fig. 5*A*). When mice were immunized with sorted FCs, tumor growth was similarly inhibited as immunized with FCs, and the inhibition of tumor growth was also enhanced with CpG ODN (Fig. 5*A*). Mice vaccinated with FCs + CpG significantly increased survival times. Eighty percent of mice vaccinated with FCs + CpG were alive 60 days after tumor challenge, while only 20% of mice immunized with FCs alone were still alive and all mice in the other groups died (Fig. 5*B*). Furthermore, 6 of 10 mice vaccinated with FCs + CpG remained tumor free 60 days after tumor injection, whereas none of the mice immunized with FCs alone was tumor free in the B16BL6 tumor model (Fig. 5*C*).

We also examined the effect of vaccination with FCs + CpG on the enhancement of tumor-specific immunity against murine RENCA tumors in which TAAs have not been identified (Fig. 6). Mice vaccinated with FCs generated from DCs and RENCA cells had greater IFN-γ secretion than mice immunized with the mixture without fusion (Mix). IFN-γ secretion was enhanced by coadministration with CpG ODN (Fig. 6*A*). Tumor-specific CTLs were also generated and the highest cytolytic activity was obtained by vaccination with FCs + CpG (Fig. 6, *B* and *C*). Sixty days after tumor challenge with RENCA cells, 8 of 10 mice vaccinated with FCs + CpG were tumor free, while 5 of 10 mice immunized with FCs alone were tumor free and no mice from the other vaccination groups were tumor free (Fig. 6*D*). Similar results were obtained in two other experiments (Table I, Tumor-free mice/mice 1st challenged).

Therefore, immunization with FCs + CpG strongly induced Th1 cytokines and activated tumor-specific CTLs, resulting in the

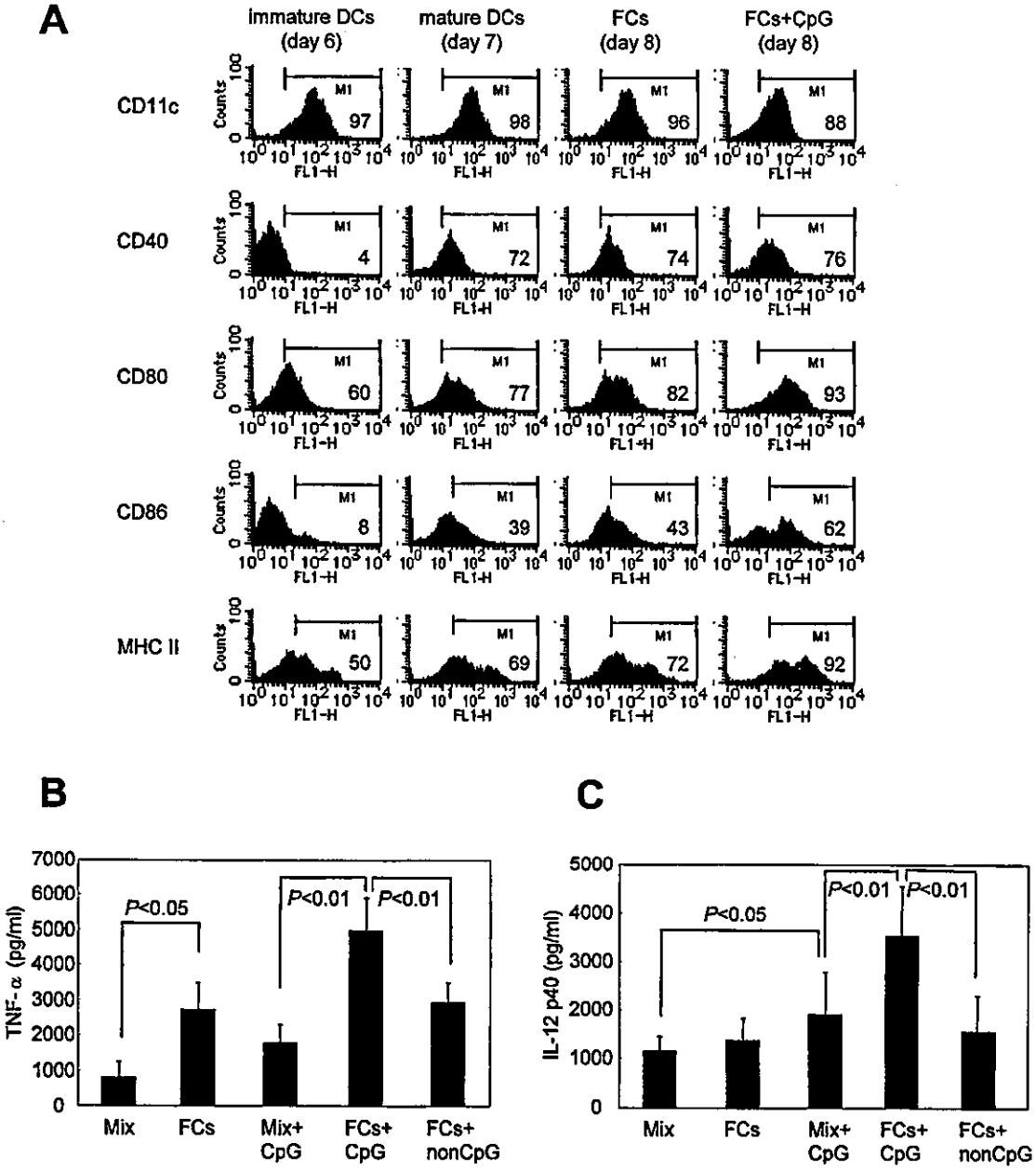

FIGURE 3. Enhanced phenotypical maturation and Th1 cytokine production of FCs in combination with CpG ODN in vitro. *A*, Surface phenotype. After 24-h incubation of fusion products with (FCs + CpG) or without (FCs) 10 μg/ml CpG ODN, surface phenotypes of DC-tumor FCs were gated and analyzed by flow cytometry. Phenotypes of immature and LPS-prestimulated mature DCs are shown as controls. Each number indicates the percentage of positive cells. These experiments were repeated twice with similar results. *B* and *C*, Th1 cytokine production. TNF-α (*B*) and IL-12 p40 (*C*) in the supernatants of either mixture (Mix) of DCs and tumor cells or DC-tumor FCs were measured with ELISA kits. The effect of 10 μg/ml CpG ODN on cytokine production was assessed. Non-CpG ODN were used as a control. Data are presented as the mean ± SD of four independent experiments.

significantly sufficient protection against B16BL6 tumors, in which TAAs have been identified, and RENCA tumors, in which TAAs are unknown.

Inhibition of lung metastasis by FCs in combination with CpG ODN

The effect of vaccination with FCs + CpG on the inhibition of lung metastasis was further investigated. B16BL6 cells were injected into the right hind footpad of vaccinated mice. On day 21 after tumor inoculation, the primary tumor was surgically removed. All mice were euthanized 21 days after surgery, and the number of lung metastases of melanoma was counted in the eight mice. The number of metastatic foci was significantly reduced by vaccination with FCs (Fig. 7). Moreover, mice immunized with FCs + CpG further inhibited lung metastases as compared with either FCs alone or Mix + CpG (Fig. 7).

Enhanced long-lasting immune response of FCs by coadministration with CpG ODN

Our results indicated that CpG ODN strongly enhanced tumor-specific immune response of FCs. We finally investigated whether CpG ODN maintain tumor-specific immunity of FCs. Six of 10 mice in the B16BL6 tumor model and 8 of 10 mice in the RENCA tumor model that received vaccination with FCs + CpG remained tumor free for 60 days after the first tumor injection (Figs. 5*C* and 6*D*). These mice were rechallenged with the same tumor cells used

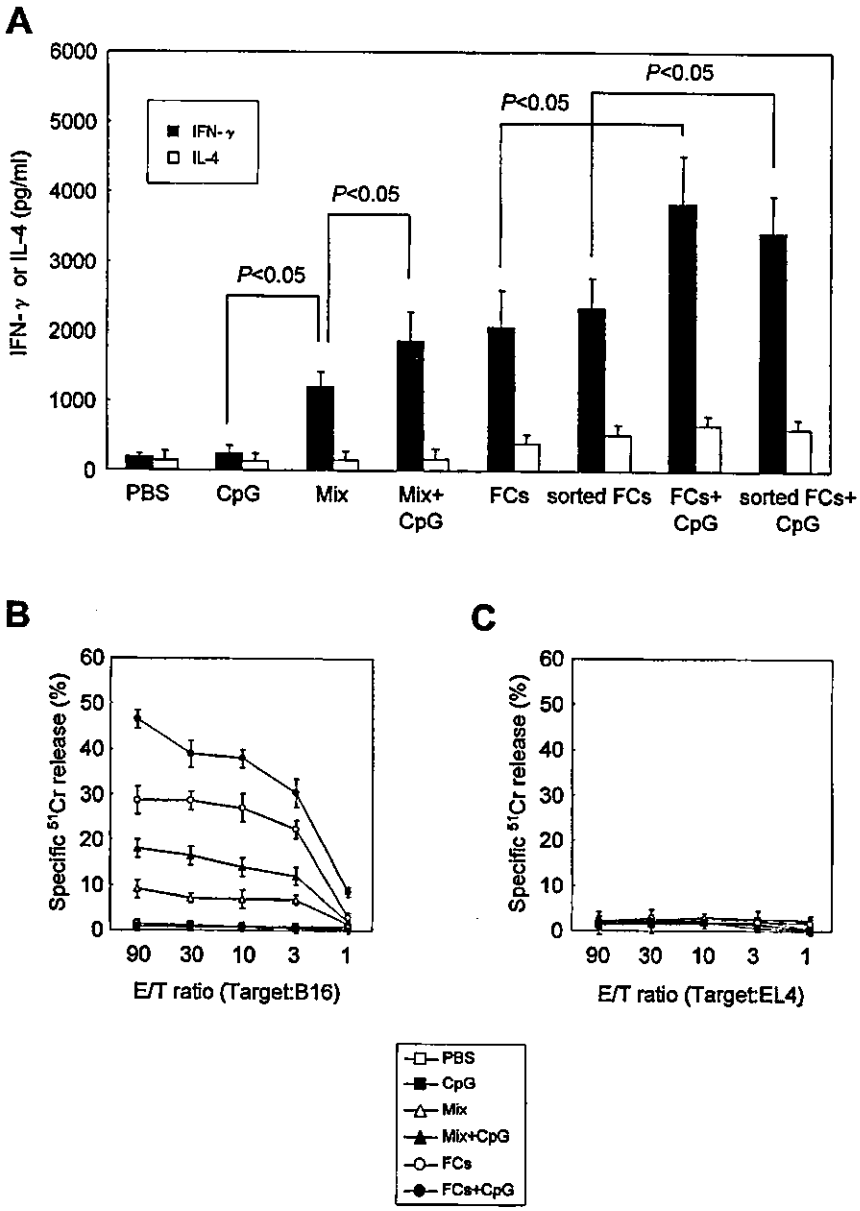

FIGURE 4. Enhanced B16BL6 cell-specific immune response of FCs coinjected with CpG ODN in vivo. *A*, IFN-γ and IL-4 production. Mice vaccinated with either FCs + CpG or sorted FCs + CpG had significantly higher IFN-γ concentration in the supernatants from spleen cell cultures on day 5 during restimulation. Data are presented as the mean ± SD of three independent experiments. *B* and *C*, Cytolytic assay. Ten days after the second immunization, spleen cells isolated from vaccinated mice were cocultured with mitomycin C-treated B16BL6 cells for 5 days and used as effector cells in 4-h ^{51}Cr release assay. Significantly higher cytolytic activity was observed in the mice that received FCs + CpG (*B*), whereas no cytolytic effect was observed when EL4 cells were used as the target cells (*C*). Data are presented as the mean ± SD of triplicate samples of one representative experiment. These experiments were repeated twice with similar results.

for the first challenge or with other syngeneic tumor cells. All mice immunized with FCs + CpG completely rejected tumor rechallenge with the same tumor cells (B16BL6 or RENCA cells) and remained tumor free for 60 days after the second tumor injection (Table I), while the mice did not reject other syngeneic tumor cells (EL4 or CT26 cells). However, among five BALB/c mice that rejected the first tumor challenge with RENCA cells by immunization with FCs alone (Fig. 6*D*), only two mice rejected tumor rechallenge with the same tumor cells and three mice developed RENCA tumors (Table I, Expt. 1). Similar results were obtained in two other experiments (Table I). These findings indicate that CpG ODN could enhance long-lasting tumor-specific immunity generated by FCs. FCs in the absence of CpG ODN did not maintain tumor-specific immunity so effectively as FCs + CpG ODN, resulting in incomplete protection against tumor rechallenge.

Discussion

In this study, we demonstrated that a new vaccination strategy of HVJ-mediated DC-tumor FCs in combination with CpG ODN induced tumor-specific and long-term immunity against two different murine tumors.

A number of studies have reported that DC-tumor FCs induce tumor-specific immune response (7–12). These studies suggested that the effective presentation of both known and unknown TAAs is feasible with DC-tumor FCs. Our study also supports the utility of DC-tumor cell fusion for eliciting antitumor immunity. In this study, we used inactivated HVJ as a fusogen. Under optimal fusion conditions, HVJ generated 20–30% of DC-tumor FCs with low toxicity, accompanied by few or no DC-DC or tumor-tumor FCs (Fig. 1, *A* and *B*). The fusion efficiency using HVJ was comparable to the previously reported fusion efficiency of PEG (7–10) and electrofusion (11, 12). However, in our hands, fusion efficiency between DC and tumor cells and the viability of FCs using PEG was very low (<10 and 40%, respectively). The PEG fusion method is technically challenging. It has been reported that it is difficult to determine optimal conditions for effective electrofusion with low toxicity (11, 12). Thus, HVJ-mediated cell fusion appeared to be simpler and more reproducible than other fusion methods.

Two distinct glycoproteins of HVJ are required for cell fusion (26). Hemagglutinin neuraminidase protein binds to sialic acid receptors on the cell surface and degrades the receptor by sialidase

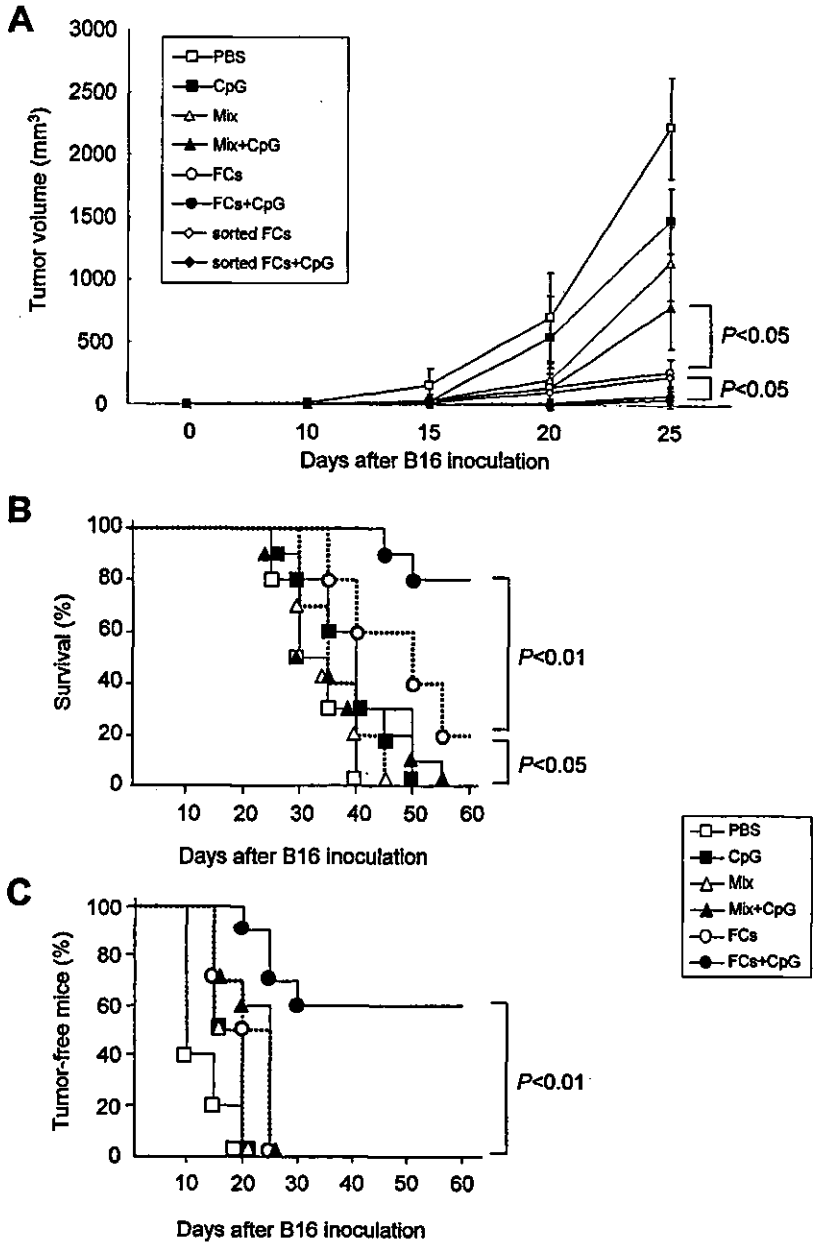

FIGURE 5. Inhibition of melanoma growth in mice using FCs combined with CpG ODN. The antitumor effect of the vaccinations with CpG ODN in combination with the mixture of DCs and tumor cells (Mix) or DC-tumor FCs was examined in the prophylactic model. C57BL/6 mice (10 mice per group) were pre-immunized twice i.d. with PBS (□), CpG ODN (■), Mix (△), Mix + CpG (▲), FCs (○), FCs + CpG (●), sorted FCs (◇), or sorted FCs + CpG (◆). Ten days after the second immunization, these mice were challenged by s.c. injection of 1×10^5 B16BL6 cells into the back on day 0. *A*, The growth of B16BL6 after s.c. inoculation into vaccinated mice. Data are presented as the mean tumor volume ± SD. *B*, The percentage of surviving mice after tumor injection. *C*, The ratio of tumor-free mice after tumor injection. These experiments were repeated twice with similar results.

activity. Fusion protein then associates with lipid molecules, such as cholesterol, on the cell surface to induce cell fusion. Recently, Phan et al. (32) developed a new method to generate DC-tumor FCs based on gene transfer of a fusogenic glycoprotein derived from vesicular stomatitis virus into tumor cells. This report supports our DC-tumor cell fusion method using viral fusion proteins, such as hemagglutinin neuraminidase and fusion proteins, of HVJ.

DC-tumor FCs possess properties that include both known and unknown TAAs derived from tumor cells, as well as necessary levels of MHC, costimulatory molecules, and probably other components derived from DCs (Fig. 2, *A* and *B*). The rationale for using DC-tumor FCs as a cancer vaccine is to raise T cells directed against the whole antigenic repertoire of the tumor cells (6). Because tumors escape from immunosurveillance through the down-regulation of MHC class I or TAA expression (36), it is likely that successful vaccination for immunotherapy or immunoprevention against tumors requires multiple tumor Ags like a polyvalent vaccine (37). DC-tumor FCs appear to be ideal cancer vaccines because various kinds of TAAs can be presented by MHC class I molecules derived from DCs, even though tumor cells lose the expression of MHC class I molecules and some TAAs (6, 38).

Because it is necessary to trigger innate immunity for subsequent effective acquired immunity (20), we attempted to enhance the antitumor activity induced by immunization with DC-tumor FCs by using CpG ODN as an adjuvant. CpG ODN are recognized by TLR9 mainly in DCs, leading to activation of the innate immune system, which includes DCs, macrophages, and NK cells (20). Because DC-tumor FCs possessed properties of both DCs and tumor cells (Fig. 2*B*), we expected that TLR9 expressed in DCs could also be expressed in DC-tumor FCs, and therefore, CpG ODN could directly stimulate these cells. Indeed, we found that CpG ODN enhanced the phenotypical maturation and Th1 cytokine production of FCs, but not of the mixture without fusion, indicating that FCs themselves might be activated by CpG ODN through TLR9.

We observed that repeated i.d. administration of CpG ODN alone was safe, but failed to protect mice against subsequent tumor challenge as previously reported (39), indicating that, especially in

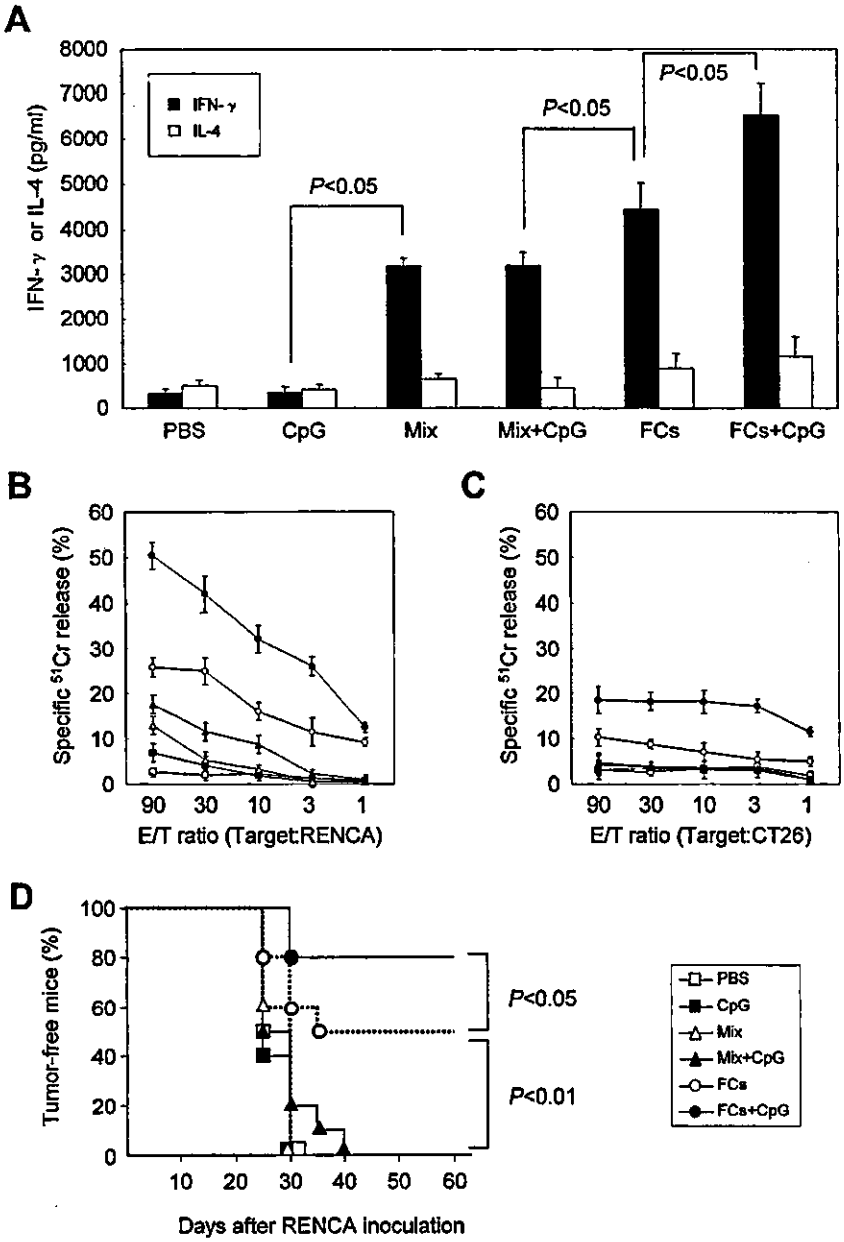

FIGURE 6. Enhanced RENCA cell-specific immune response of FCs by coadministration with CpG ODN in vivo. BALB/c mice (10 mice per group) were preimmunized twice i.d. with PBS (□), CpG ODN (■), Mix (△), Mix + CpG (▲), FCs (○), or FCs + CpG (●). Ten days after the second immunization, these mice were challenged by s.c. injection of 1×10^5 RENCA cells into the back on day 0. *A*, IFN-γ and IL-4 production. The mice that received FCs + CpG vaccination had significantly higher IFN-γ concentration in the supernatants from spleen cell cultures on day 5 during restimulation. Data are presented as the mean ± SD of three independent experiments. *B* and *C*, Cytolytic assay. Cytolytic activity was assessed by specific ^{51}Cr release from RENCA cells (*B*) and CT26 cells (*C*). Data are presented as the mean ± SD of triplicate samples of one representative experiment. *D*, The ratio of tumor-free mice after the injection of RENCA cells. These experiments were repeated three times with similar results.

prophylactic use, CpG ODN alone induce only nonspecific expansion of the innate immune cells (40). In contrast, we demonstrated that i.d. immunization with FCs, but not the mixture of DCs and tumor cells, induced higher tumor-specific cytolytic activity and provided significant protection against tumor challenge. We found that vaccination with fusion products generated from either DCs alone, which contain DC-DC FCs, or tumor cells alone, which contain tumor-tumor FCs, did not protect mice (data not shown).

Table I. *Complete induction of tumor-specific long-term immunity after tumor rechallenge in mice immunized with FCs plus CpG ODN*[a]

Mice	Tumor Cell 1st Challenged	Preimmunization Tumor-Free Mice/ Mice 1st Challenged[b]	Tumor Cell 2nd Challenged	Tumor-Free Mice/Mice 2nd Challenged[c]
C57/BL6	B16	**FCs**		
		0/10 (0%), 0/10 (0%), 0/10 (0%)		
		FCs + CpG	B16	3/3 (100%), 2/2 (100%), 3/3 (100%)
		6/10 (60%), 4/10 (40%), 5/10 (50%)	EL4	0/3 (0%), 0/2 (0%), 0/2 (0%)
BALB/c	RENCA	**FCs**	RENCA	2/5 (40%), 3/6 (50%), 1/4 (25%)
		5/10 (50%), 6/10 (60%), 4/10 (40%)		
		FCs + CpG	RENCA	4/4 (100%), 5/5 (100%), 3/3 (100%)
		8/10 (80%), 9/10 (90%), 6/10 (60%)	CT26	0/4 (0%), 0/4 (0%), 0/3 (0%)

[a] This table represents the results of three independent experiments (Expt. 1, Expt. 2, Expt. 3).
[b] The ratio of tumor-free mice on day 60 after the first tumor challenge.
[c] The ratio of tumor-free mice on day 60 after the second tumor challenge.

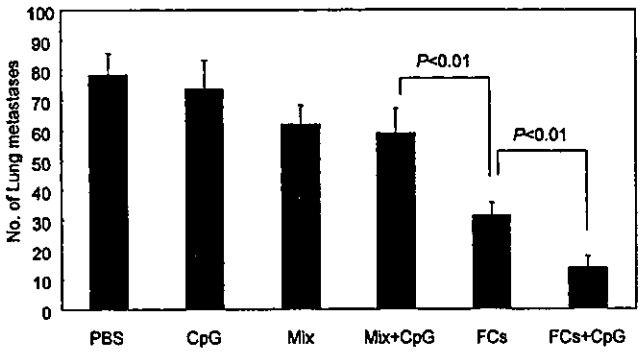

FIGURE 7. Inhibition of lung metastasis by FCs in combination with CpG ODN. The effect of various vaccinations on the inhibition of lung metastasis was investigated. Ten days after the second vaccination, C57BL/6 mice (eight mice per group) were s.c. injected with 5×10^5 B16BL6 cells into the right hind footpad. On day 21 after tumor inoculation, the primary tumor was surgically removed. All mice were euthanized 21 days after surgery, and the number of lung metastatic foci in each mouse is shown. Data are presented as the mean ± SD of three independent experiments.

Additionally, in the combination with or without CpG ODN, antitumor activity of 6×10^6 FCs containing both fused and unfused cells was comparable to that of 1.2×10^6 sorted FCs (Figs. 4*A* and 5*A*). These findings indicate that DC-tumor FC fraction, which only exists in the FCs, is required to elicit the antitumor effect. Moreover, we revealed that i.d. immunization with CpG ODN in combination with FCs, but not with the mixture, further enhanced tumor-specific immune response generated by FCs. CpG ODN might enhance cross-presentation of TAAs by both FCs (38) and unfused DCs (41), leading to effective activation of MHC class I-restricted CTLs. The results of cytolytic assay indicate that $CD8^+$ CTLs are mainly involved in the tumor-specific cytolytic activity, at least through IFN-γ release induced by the vaccination with FCs in combination with or without CpG ODN. However, cytolytic activity against CT26 cells was observed in spleen cells from the mice vaccinated with FCs between DCs and RENCA tumor cells in combination with CpG ODN (Fig. 6*C*), although the activity was much lower than that against RENCA cells. This result suggests that NK cells might also participate in this response to some extent. This speculation is supported by previous reports showing that both $CD8^+$ and NK cells (29, 30), in addition to $CD4^+$ cells (7), are activated by the immunization with FCs between DCs and tumor cells, and that both $CD8^+$ and NK cells mediate CpG ODN-induced antitumor immune response (42).

We demonstrated that CpG ODN provided long-term maintenance of tumor-specific immunity induced by FCs, leading to complete rejection of tumor rechallenge (Table I). Although the precise mechanisms by which CpG ODN are capable of maintaining the antitumor effect generated by FCs are unknown, several possibilities can be explored. Effective antitumor immunity generally requires $CD4^+$ Th cells, which participate in further activation of DCs through CD40-CD40L interaction and subsequent induction of $CD8^+$ effector CTL response (1). However, it is also indicated that effector CTLs can be induced without $CD4^+$ Th cells (43). The induction of $CD4^+$ Th cell-independent CTL function may also occur in DC-tumor FC vaccines. However, in terms of maintenance after the induction of effector CTLs, recent studies have reported that $CD4^+$ T cell help plays a critical role in the development and activation of functional $CD8^+$ memory T cells (44, 45). It has also been recently reported that CpG ODN not only enhance but also maintain $CD8^+$ effector CTL response through the expansion, inhibition of apoptosis, and subsequent promotion of long-term survival of $CD8^+$ effector and memory T cells (40, 46). Especially, the expansion and survival of memory $CD8^+$ T cells have been reported to be mediated by IL-15 (47), which is produced by DCs in response to type I IFN (48). CpG ODN stimulate DCs to produce type I IFN (49). Taken together, we estimated that in our experiments, $CD4^+$, $CD8^+$, and NK cells would play a key role in the activation and enhancement of long-lasting tumor-specific immune response by the immunization with FCs + CpG ODN.

Moreover, the generation of humoral response against tumors using hybrid cell vaccine has been already reported in several papers (9, 50), and the significance of antimelanoma Ab after the injection of TAA genes has been also reported (51). Therefore, it is estimated that the humoral response against tumors might be also induced by the vaccination with FCs or FCs + CpG ODN.

From the viewpoint of cancer immunoprevention, this combination vaccine is ideal because the presentation of many MHC-restricted known and unknown TAAs or Ags presented by the MHC-independent pathway on FCs as well as the long-lasting effect of CpG ODN on tumor-specific immunity are very useful to avoid the selection of TAA-loss variants and to recognize MHC-loss variants in the generation and recurrence of cancer (52).

In the surviving mice immunized twice with FCs in combination with CpG ODN and challenged with B16BL6 cells, no apparent inflammation, such as autoimmune skin depigmentation (vitiligo), was observed. Only localized hair loss in the area surrounding the tumor injection site was observed. Similar findings were observed in the surviving mice from the RENCA tumor model. These findings suggest that repeated vaccinations with FCs in combination with CpG ODN are safe and feasible for clinical immunotherapy and immunoprevention against cancers. This safety is essential for clinical use as a cancer immunoprevention vaccine.

In conclusion, we have developed a simple and reproducible method to generate DC-tumor FCs using inactivated HVJ. Vaccination of HVJ-mediated DC-tumor FCs in combination with CpG ODN induced tumor-specific and long-term immunity in the prophylactic setting of a s.c. tumor model and a spontaneous lung metastasis model, resulting in significant inhibition of tumor incidence and prolongation of survival time. CpG ODN could strongly enhance and maintain tumor-specific immune response induced by DC-tumor FC vaccines in vivo. We hope that this type of immunoprevention can eventually be tested in human clinical trials to inhibit cancer recurrence and micrometastasis after surgery.

References

1. Banchereau, J., and R. M. Steinman. 1998. Dendritic cells and the control of immunity. *Nature 392:245.*
2. Pardoll, D. M. 1998. Cancer vaccines. *Nat. Med. 4:525.*
3. Boon, T., J. C. Cerottini, B. Van den Eynde, P. van der Bruggen, and A. Van Pel. 1994. Tumor antigens recognized by T lymphocytes. *Annu. Rev. Immunol. 12:337.*
4. Nestle, F. O., S. Alijagic, M. Gilliet, Y. Sun, S. Grabbe, R. Dummer, G. Burg, and D. Schadendorf. 1998. Vaccination of melanoma patients with peptide- or tumor lysate-pulsed dendritic cells. *Nat. Med. 4:328.*
5. Kawakami, Y., and S. A. Rosenberg. 1997. Human tumor antigens recognized by T-cells. *Immunol. Res. 16:313.*
6. Kufe, D. W. 2000. Smallpox, polio and now a cancer vaccine? *Nat. Med. 6:252.*
7. Gong, J., D. Chen, M. Kashiwaba, and D. Kufe. 1997. Induction of antitumor activity by immunization with fusions of dendritic and carcinoma cells. *Nat. Med. 3:558.*
8. Wang, J., S. Saffold, X. Cao, J. Krauss, and W. Chen. 1998. Eliciting T cell immunity against poorly immunogenic tumors by immunization with dendritic cell-tumor fusion vaccines. *J. Immunol. 161:5516.*
9. Gong, J., S. Koido, D. Chen, Y. Tanaka, L. Huang, D. Avigan, K. Anderson, T. Ohno, and D. Kufe. 2002. Immunization against murine multiple myeloma with fusions of dendritic and plasmacytoma cells is potentiated by interleukin 12. *Blood 99:2512.*

10. Chan, R. C., H. Xie, G. P. Zhao, and Y. Xie. 2002. Dendritomas formed by fusion of mature dendritic cells with allogenic human hepatocellular carcinoma cells activate autologous cytotoxic T lymphocytes. *Immunol. Lett. 83:101.*
11. Hayashi, T., H. Tanaka, J. Tanaka, R. Wang, B. J. Averbook, P. A. Cohen, and S. Shu. 2002. Immunogenicity and therapeutic efficacy of dendritic-tumor hybrid cells generated by electrofusion. *Clin. Immunol. 104:14.*
12. Siders, W. M., K. L. Vergilis, C. Johnson, J. Shields, and J. M. Kaplan. 2003. Induction of specific antitumor immunity in the mouse with the electrofusion product of tumor cells and dendritic cells. *Mol. Ther. 7:498.*
13. Kikuchi, T., Y. Akasaki, M. Irie, S. Homma, T. Abe, and T. Ohno. 2001. Results of a phase I clinical trial of vaccination of glioma patients with fusions of dendritic and glioma cells. *Cancer Immunol. Immunother. 50:337.*
14. Krause, S. W., C. Neumann, A. Soruri, S. Mayer, J. H. Peters, and R. Andreesen. 2002. The treatment of patients with disseminated malignant melanoma by vaccination with autologous cell hybrids of tumor cells and dendritic cells. *J. Immunother. 25:421.*
15. Lutz, M. B., and G. Schuler. 2002. Immature, semi-mature and fully mature dendritic cells: which signals induce tolerance or immunity? *Trends Immunol. 23:445.*
16. Parmiani, G., C. Castelli, P. Dalerba, R. Mortarini, L. Rivoltini, F. M. Marincola, and A. Anichini. 2002. Cancer immunotherapy with peptide-based vaccines: what have we achieved? Where are we going? *J. Natl. Cancer Inst. 94:805.*
17. Krieg, A. M. 2003. CpG motifs: the active ingredient in bacterial extracts? *Nat. Med. 9:831.*
18. Krieg, A. M., A. K. Yi, S. Matson, T. J. Waldschmidt, G. A. Bishop, R. Teasdale, G. A. Koretzky, and D. M. Klinman. 1995. CpG motifs in bacterial DNA trigger direct B-cell activation. *Nature 374:546.*
19. Weeratna, R. D., M. J. McCluskie, Y. Xu, and H. L. Davis. 2000. CpG DNA induces stronger immune responses with less toxicity than other adjuvants. *Vaccine 18:1755.*
20. Akira, S., K. Takeda, and T. Kaisho. 2001. Toll-like receptors: critical proteins linking innate and acquired immunity. *Nat. Immunol. 2:675.*
21. Heckelsmiller, K., S. Beck, K. Rall, B. Sipos, A. Schlamp, E. Tuma, S. Rothenfusser, S. Endres, and G. Hartmann. 2002. Combined dendritic cell- and CpG oligonucleotide-based immune therapy cures large murine tumors that resist chemotherapy. *Eur. J. Immunol. 32:3235.*
22. Baines, J., and E. Celis. 2003. Immune-mediated tumor regression induced by CpG-containing oligodeoxynucleotides. *Clin. Cancer Res. 9:2693.*
23. Jiang, W., and D. S. Pisetsky. 2003. Enhancing immunogenicity by CpG DNA. *Curr. Opin. Mol. Ther. 5:180.*
24. Inaba, K., M. Inaba, N. Romani, H. Aya, M. Deguchi, S. Ikehara, S. Muramatsu, and R. M. Steinman. 1992. Generation of large numbers of dendritic cells from mouse bone marrow cultures supplemented with granulocyte/macrophage colony-stimulating factor. *J. Exp. Med. 176:1693.*
25. Kaisho, T., O. Takeuchi, T. Kawai, K. Hoshino, and S. Akira. 2001. Endotoxin-induced maturation of MyD88-deficient dendritic cells. *J. Immunol. 166:5688.*
26. Okada, Y. 1993. Sendai virus-induced cell fusion. *Methods Enzymol. 221:18.*
27. Kaneda, Y., T. Nakajima, T. Nishikawa, S. Yamamoto, H. Ikegami, N. Suzuki, H. Nakamura, R. Morishita, and H. Kotani. 2002. Hemagglutinating virus of Japan (HVJ) envelope vector as a versatile gene delivery system. *Mol. Ther. 6:219.*
28. Miyake, Y., J. Kim, and Y. Okada. 1978. Effects of cytochalasin D on fusion of cells by HVJ (Sendai virus). *Exp. Cell Res. 116:167.*
29. Orentas, R. J., D. Schauer, Q. Bin, and B. D. Johnson. 2001. Electrofusion of a weakly immunogenic neuroblastoma with dendritic cells produces a tumor vaccine. *Cell. Immunol. 213:4.*
30. Akasaki, Y., T. Kikuchi, S. Homma, T. Abe, D. Kofe, and T. Ohno. 2001. Antitumor effect of immunizations with fusions of dendritic and glioma cells in a mouse brain tumor model. *J. Immunother. 24:106.*
31. Koido, S., Y. Tanaka, D. Chen, D. Kufe, and J. Gong. 2002. The kinetics of in vivo priming of CD4 and CD8 T cells by dendritic/tumor fusion cells in MUC1-transgenic mice. *J. Immunol. 168:2111.*
32. Phan, V., F. Errington, S. C. Cheong, T. Kottke, M. Gough, S. Altmann, A. Brandenburger, S. Emery, S. Strome, A. Bateman, et al. 2003. A new genetic method to generate and isolate small, short-lived but highly potent dendritic cell-tumor cell hybrid vaccines. *Nat. Med. 9:1215.*
33. Dethlefsen, L. A., J. M. Prewitt, and M. L. Mendelsohn. 1968. Analysis of tumor growth curves. *J. Natl. Cancer Inst. 40:389.*
34. Poste, G., J. Doll, I. R. Hart, and I. J. Fidler. 1980. In vitro selection of murine B16 melanoma variants with enhanced tissue-invasive properties. *Cancer Res. 40:1636.*
35. Saiki, I., J. Iida, J. Murata, R. Ogawa, N. Nishi, K. Sugimura, S. Tokura, and I. Azuma. 1989. Inhibition of the metastasis of murine malignant melanoma by synthetic polymeric peptides containing core sequences of cell-adhesive molecules. *Cancer Res. 49:3815.*
36. Garcia-Lora, A., I. Algarra, and F. Garrido. 2003. MHC class I antigens, immune surveillance, and tumor immune escape. *J. Cell. Physiol. 195:346.*
37. Morton, D. L., L. J. Foshag, D. S. Hoon, J. A. Nizze, E. Famatiga, L. A. Wanek, C. Chang, D. G. Davtyan, R. K. Gupta, R. Elashoff, et al. 1992. Prolongation of survival in metastatic melanoma after active specific immunotherapy with a new polyvalent melanoma vaccine. *Ann. Surg. 216:463.*
38. Parkhurst, M. R., C. DePan, J. P. Riley, S. A. Rosenberg, and S. Shu. 2003. Hybrids of dendritic cells and tumor cells generated by electrofusion simultaneously present immunodominant epitopes from multiple human tumor-associated antigens in the context of MHC class I and class II molecules. *J. Immunol. 170:5317.*
39. Heckelsmiller, K., K. Rall, S. Beck, A. Schlamp, J. Seiderer, B. Jahrsdorfer, A. Krug, S. Rothenfusser, S. Endres, and G. Hartmann. 2002. Peritumoral CpG DNA elicits a coordinated response of CD8 T cells and innate effectors to cure established tumors in a murine colon carcinoma model. *J. Immunol. 169:3892.*
40. Davila, E., M. G. Velez, C. J. Heppelmann, and E. Celis. 2002. Creating space: an antigen-independent, CpG-induced peripheral expansion of naive and memory T lymphocytes in a full T-cell compartment. *Blood 100:2537.*
41. Warren, T. L., S. K. Bhatia, A. M. Acosta, C. E. Dahle, T. L. Ratliff, A. M. Krieg, and G. J. Weiner. 2000. APC stimulated by CpG oligodeoxynucleotide enhance activation of MHC class I-restricted T cells. *J. Immunol. 165:6244.*
42. Kawarada, Y., R. Ganss, N. Garbi, T. Sacher, B. Arnold, and G. J. Hammerling. 2001. NK^- and $CD8^+$ T cell-mediated eradication of established tumors by peritumoral injection of CpG-containing oligodeoxynucleotides. *J. Immunol. 167:5247.*
43. Shiku, H. 2003. Importance of $CD4^+$ helper T-cells in antitumor immunity. *Int. J. Hematol. 77:435.*
44. Janssen, E. M., E. E. Lemmens, T. Wolfe, U. Christen, M. G. von Herrath, and S. P. Schoenberger. 2003. $CD4^+$ T cells are required for secondary expansion and memory in $CD8^+$ T lymphocytes. *Nature 421:852.*
45. Gao, F. G., V. Khammanivong, W. J. Liu, G. R. Leggatt, I. H. Frazer, and G. J. Fernando. 2002. Antigen-specific $CD4^+$ T-cell help is required to activate a memory $CD8^+$ T cell to a fully functional tumor killer cell. *Cancer Res. 62:6438.*
46. Beloeil, L., M. Tomkowiak, G. Angelov, T. Walzer, P. Dubois, and J. Marvel. 2003. In vivo impact of CpG1826 oligodeoxynucleotide on CD8 T cell primary responses and survival. *J. Immunol. 171:2995.*
47. Lu, J., R. L. Giuntoli, Jr., R. Omiya, H. Kobayashi, R. Kennedy, and E. Celis. 2002. Interleukin 15 promotes antigen-independent in vitro expansion and long-term survival of antitumor cytotoxic T lymphocytes. *Clin. Cancer Res. 8:3877.*
48. Mattei, F., G. Schiavoni, F. Belardelli, and D. F. Tough. 2001. IL-15 is expressed by dendritic cells in response to type I IFN, double-stranded RNA, or lipopolysaccharide and promotes dendritic cell activation. *J. Immunol. 167:1179.*
49. Cho, H. J., T. Hayashi, S. K. Datta, K. Takabayashi, J. H. Van Uden, A. Horner, M. Corr, and E. Raz. 2002. IFN-$\alpha\beta$ promote priming of antigen-specific $CD8^+$ and $CD4^+$ T lymphocytes by immunostimulatory DNA-based vaccines. *J. Immunol. 168:4907.*
50. Xia, J., Y. Tanaka, S. Koido, C. Liu, P. Mukherjee, S. J. Gendler, and J. Gong. 2003. Prevention of spontaneous breast carcinoma by prophylactic vaccination with dendritic/tumor fusion cells. *J. Immunol. 170:1980.*
51. Tanaka, M., Y. Kaneda, S. Fujii, T. Yamano, K. Hashimoto, S. K. Huang, and D. S. Hoon. 2002. Induction of a systemic immune response by a polyvalent melanoma-associated antigen DNA vaccine for prevention and treatment of malignant melanoma. *Mol. Ther. 5:291.*
52. Lollini, P. L., and G. Forni. 2003. Cancer immunoprevention: tracking down persistent tumor antigens. *Trends Immunol. 24:62.*

Subcellular Trafficking of Exogenously Expressed Interferon-β in Madin–Darby Canine Kidney Cells

MASATO MARUYAMA,[1] TERUKO NISHIO,[1] TAKAKO KATO,[1] TOYOKAZU YOSHIDA,[1] CHISAKI ISHIDA,[1] YOSHIHIKO WATANABE,[2] MAKIYA NISHIKAWA,[1] YASUFUMI KANEDA,[3] AND YOSHINOBU TAKAKURA[1]*

[1]*Department of Biopharmaceutics and Drug Metabolism, Graduate School of Pharmaceutical Sciences, Kyoto University, Sakyo-ku, Kyoto, Japan*

[2]*Department of Molecular Microbiology, Graduate School of Pharmaceutical Sciences, Kyoto University, Sakyo-ku, Kyoto, Japan*

[3]*Division of Gene Therapy Science, Osaka University, School of Medicine, Suita, Osaka, Japan*

We have recently demonstrated that when IFN-β was exogenously expressed in epithelial cells, transiently expressed IFN-β was predominantly secreted from the cell side to which the transfection was performed, while stably expressed one was almost equally secreted to the apical and basolateral sides. In the present study, we analyzed the subcellular transport of IFN-β using confocal imaging with green fluorescent protein (GFP)-tagged IFN-β in Madin–Darby canine kidney (MDCK) cells. Stably expressed and transiently expressed human IFN-β (HuIFN-β)–GFPs were seen in upper regions of the nucleus. In stable HuIFN β–GFP-producing transformants, transiently expressed mouse IFN-β (MuIFN-β) was apparently co-localized with the bulk of the constitutive HuIFN β–GFP proteins at TGN, and a significant quantity of them then appeared to pass into distinct post-TGN vesicles, accepting either type of IFN. Meanwhile, when cells were co-transfected with both expression vectors, transiently expressed both IFNs tended to co-localize not only at TGN but in post-TGN vesicles. These results suggest that stably and transiently expressed IFN-βs, albeit co-localized at TGN, were transported through apparently discriminated post-TGN routes. J. Cell. Physiol. 201: 117–125, 2004.

In polarized epithelial cells, the surface membrane is divided by the tight junctions (TJ) into apical and basorateral domains, which have different lipid and protein compositions (Rodriguez-Boulan and Nelson, 1989). This domain structure is maintained by specialized vectorial transport of the components. Newly synthesized domain-specific membrane proteins are conveyed through the endoplasmic reticulum (ER)-Golgi apparatus to the trans-Golgi network (TGN) (Keller and Simons, 1997), and packaged into transport carriers for membrane integration (Griffiths and Simons, 1986). The destination of the membrane proteins seems to be determined by interrelation between some signal sequences on the protein and various cellular components playing roles in sorting and trafficking (Wandinger-Ness et al., 1990). Secretory proteins are also considered to be transported in the same manner as the membrane proteins (Lippincott-Schwartz et al., 2000). In spite of many investigations of the issue, the mechanisms regulating apical or basolateral sorting of secretory proteins remain elusive.

The green fluorescent protein (GFP) of the jellyfish *Aequorea victoria* (Tsien, 1998) and its variants are widely used in cell imaging applications (Lippincott-Schwartz and Patterson, 2003) to reveal the location of proteins. Results from those applications are providing new insights into protein function and cellular processes in the complex environment of the cell. The GFP-tagging technology is useful for directly investigating the intracellular localization, movement and fate of secretory proteins of interest in living cells.

We have recently examined the mode of secretion polarity of interferon (IFN)-β expressed exogenously in several epithelial cell lines (Nakanishi et al., 2002) or by stimulation with a type I IFN inducer, polyriboinosinic

Contract grant sponsor: Scientific Research from the Ministry of Education, Cultures, Sports, Science, and Technology, Japan.

*Correspondence to: Yoshinobu Takakura, Department of Biopharmaceutics and Drug Metabolism, Graduate School of Pharmaceutical Sciences, Kyoto University, Sakyo-ku, Kyoto 606-8501, Japan. E-mail: takakura@pharm.kyoto-u.ac.jp

Received 8 September 2003; Accepted 9 December 2003

Published online in Wiley InterScience (www.interscience.wiley.com.), 27 February 2004.
DOI: 10.1002/jcp.20038